Investigation of the reaction between mould slag inclusions and high aluminium steels in the continuous caster

Innovation report

Akalya Raviraj

Doctor of Engineering in Sustainable Materials and Manufacturing

CDT for Sustainable Materials and Manufacturing, WMG, University of Warwick

This thesis is submitted in partial fulfilment of the requirements for the degree of EngD in Sustainable materials and manufacturing.

WMG, University of Warwick

Academic Mentors: Dr Stephen Spooner, Prof. Claire Davis, Prof. Mark Williams

Prof. Sridhar Seetharaman

Industrial Mentor: Dr Wouter Tiekink, Mr Gert Abbel

April 2021

Declaration

This thesis is submitted in support of my application for the degree of Doctor of Engineering. No substantial part of the work submitted here has also been submitted by me in other assessments for this or previous degree courses. The work presented (including data generated and data analysis) was carried out by the author except in the case outlined below:

- X-ray Computed Tomography scanning was carried out by Dr Jay Warnett and Dr Nadia Kourra.

Akalya Raviraj, March 2021

Abstract

Mould slag entrainment during the continuous casting process presents a late-stage source of non-metallic inclusions (NMI) with a high likelihood of ending up in the final steel product. The reaction between the entrained slag phase and surrounding liquid steel in the continuous casting mould affects the inclusion morphology and properties. The changes in composition can have adverse effects with the viscosity and heat transfer properties of the mould flux. However, there is a lack of information on the kinetics of the NMI-steel reaction. Using a controlled synthetic inclusion and metal samples, the interaction between inclusion-slag droplets and steel can be investigated to study the reaction and any change in morphology of the inclusion.

Using a correlative approach combining High-Temperature Confocal Scanning Laser Microscopy (HT-CSLM), X-ray Computed Tomography (XCT) and advanced electron microscopy techniques offers the ability to observe the size, shape and composition of an unconstrained reacting inclusion within the steel matrix without dissolving the steel. To investigate this, a low aluminium steel (0.04 wt. %) and a high aluminium steel (1 wt. %) in contact with an inclusion-slag phase with a starting composition aligned to a typical silica-rich mould slag. It was found that the reaction between silica and aluminium across the interface of the two phases provided a driving force for spontaneous emulsification of the inclusion to occur.

Further tests were carried out with an inclusion particle positioned in a dimple on the surface of the steel heated to different temperatures (representing conditions of solid inclusion – solid steel; liquid inclusion – solid steel; and liquid inclusion – semi-solid steel to calculate reaction times that could be present in the continuous caster as the steel slab is cooling.

A mathematical model has also been developed to calculate the kinetics of the reaction by using Gibbs Free energy to calculate the equilibrium constant and the compositions of the components at equilibrium. It has been found that the emulsification of inclusions will have an effect on the floatation rate and potential inclusion removal can be up to 11% longer if spontaneous emulsification were to occur in the continuous caster. Battery cans with inclusions were also investigated and characterised to define a potential pathway for these defects to occur.

The knowledge created has a great impact as inclusions affect all grades of steel, which results in huge losses of yield. Improving any aspect of the yield will have an enormous effect on sustainability due to steel manufacturing being extremely energy intrusive and having a large carbon footprint. The steels used in this study AHSS (Advanced High Strength Steel) including TRIP (Trans- formation Induced Plasticity) steel and DP (Dual Phase) steel are becoming prevalent for their low cost and high strength characteristics.

Acknowledgements

I have been extremely lucky to complete a doctorate thesis under an amazing supervision team. Without their help, this thesis and my EngD would not have come to fruition.

I would like to thank Dr Stephen Spooner for his assistance and stoic patience at every stage of this research project. Thank you for all the endless of hours, insight and tuition in all areas of steelmaking, chemistry and reaction kinetics. His innovative ideas and questions that encourage original thinking and initiative have been truly appreciated.

Thank you to Professor Claire Davis for her motivation and immense knowledge for the project. I am gratefully indebted to her, for all the valuable guidance and comments throughout the duration of the project. Her enthusiasm and positivity are contagious. Her meticulous scrutiny and attention to detail have driven me to write this thesis to the best of my ability.

I would like to thank Professor Mark Williams for all his words of wisdom and guidance over the last four years. His advice on project management and the importance of structure has been integral to the completion of this doctorate. Thank you for always making the time to chat with me and for always encouraging me to present and publish my research.

Thank you to Professor Sridhar Seetharaman whose dedication and keen interest and above all, his overwhelming effort to help his students has been truly appreciated. His timely and scholarly advice and scientific approach have helped me to a great extent to complete this doctorate. Despite being at another university in another country, he remained invested in the quality and outcome of my work.

I have been very fortunate to work with Dr Wouter Tiekink and Mr Gert Abbel from Tata Steel Europe who have been my industrial mentors. They have always been so welcoming whenever I have visited their site. They have been a huge part of this thesis for giving me perspective on where this research fits into the bigger picture and its relevance industrially. Their knowledge on inclusions and steel reactions was an invaluable resource during this EngD.

My deepest gratitude goes to colleagues at WMG, University of Warwick, past and present, to name a few, Dr Nadia Kourra, Dr Kateryna Hechu, Dr Mo Ji, Dr Juncheng Li, Dr Carl Slater, Dr Hiren Kotadia, Dr Russell Hall, Dr Jason Warnett, Mr Darbaz Khasraw, Miss Theint Theint Htet, Miss Chloe Patel, Mr Oba Waiyaki and Miss Rebecca Mackley. I appreciate each and every one of you for always taking the time to have chats, countless coffees and advice about doctorate life and careers. I would also like to thank Dr Geoff West, Dr Sabrina Yan, Mr Stephen Hewitt and Mr Michael Green for all their technical support and training in the laboratories. I would also like to thank Ms Sue Gibson,

administrator of the Sustainable Materials and Manufacturing CDT, for her unwavering support with all aspects of the EngD programme.

I would like to thank EPSRC and Tata Steel Europe for funding this research via the EngD scheme, to WMG for the provision of facilities and to Tata Steel Europe for providing the samples used in this project.

I am extremely lucky to have a wonderful support network of family and friends. I would like to thank my parents for supporting me throughout my many years in education and my brothers, Ahilan and Jeeva, for being my unfailing source of encouragement. Thank you to James for his love and support for keeping me motivated to complete this doctorate and for not letting me give up. To my friends for always being there and keeping me sane, I could not have done this without you.

Table of Contents

List of Figures

List of Tables

Frequently used abbreviations

°C	Degrees centigrade
2D	Two dimensional
3D	Three dimensional
A	Surface area
AHSS	Advanced High Strength Steel
Al	Aluminium
Al_2O_3	Alumina
BF	Blast Furnace
BOF	Basic Oxygen Furnace
CFD	Computational Fluid Dynamics
CIP CC	low carbon carbonyl iron powder
C_{slag}	Concentration of slag (wt. %)
C_{steel}	Concentration of steel (wt. %)
DP	Dual phase
EAF	Electric Arc Furnace
EBSD	Electron backscatter diffraction
EDM	Electrical discharging machine
EDS	Energy dispersive spectroscopy
Eqn.	Equation
HT-CLSM	High-Temperature Confocal Scanning Laser Microscopy
J_{steel}	Mass transfer of steel
K	Kelvin
kV	Kilovolts

LCAK	Low carbon aluminium killed
m	Metres
m/s	Metres per second
mm	Millimetres
NMI	Non-metallic inclusions
OES	Optical emission spectroscopy
PDA	Pulse discrimination analysis
ppm	Parts per million
s	Seconds
SE	Spontaneous Emulsification
SEM	Scanning Electron Microscopy
SEN	Submerged Entry Nozzle
Si	Silicon
SiO_2	Silica
TRIP	Transformation induced plasticity steel
TWIP	Twinning induced plasticity steel
USA	United States of America
VIM	Vacuum induced melting
Wt. %	Weight percentage
XCT	X-Ray Computed Tomography
μm	microns

1. Introduction

1.1 Sustainability of Steel

Steel is an extremely important material that is essential to our modern way of life, being crucial for economic growth as it is a material that is constantly being improved to meet new market demands. Steel is an alloy of carbon and iron that can be recycled many times without loss of property [16]. World crude steel production reached 1,868.8 million tonnes for the year 2019 in 65 countries, leading it to be the largest produced material in the world by weight [17,18]. Steel properties are dependent on the proportions of the alloying elements, which are closely monitored during manufacture. In steelmaking, impurities such as nitrogen, silicon, phosphorus, sulphur and excess carbon are removed from the raw hot metal produced during ironmaking [19], while alloying elements such as manganese, nickel, chromium and vanadium [20] are added to produce different grades of steel appropriate for varying applications such as electrical steels, stainless steel and automotive steels [21–23]. Steel has many favourable properties such as its high Young's modulus, outstanding combination of high strength and ductility and hence, good formability, good corrosion resistance on alloying and excellent magnetic properties. These properties are improved by alloying and controlling the structure and texture of the steel [24].

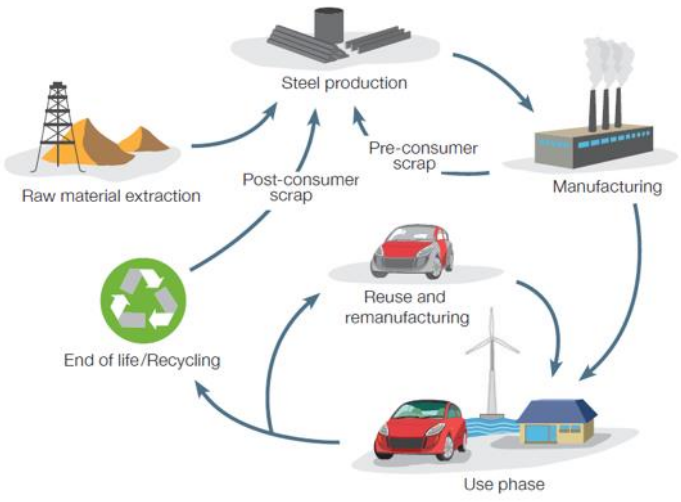

Figure 1.1 Lifecycle of steel in a green economy[1]

Steel is completely recyclable and can withstand continual recycling. It is important to recycle metals in a green economy as it preserves natural resources that are needed for primary steelmaking such as coal and iron ore and in turn requires less energy [25]. Steel is the most recycled industrial material in the world, with over 500 Mt recycled annually including pre- and post- consumer scrap [1] as shown in Figure 1.1.

Steel manufacturing has a variety of impacts on the environment as it is quite energy intensive and uses a lot of raw materials which result in emissions such as carbon dioxide, sulphur dioxides, nitrogen oxides and dust to air as well as high water usages. This makes it increasingly important to reduce impurities and defects in the steel so less steel is wasted at the end of production.

1.2 Steelmaking

Cast iron is a hard and brittle material, whereas steel is malleable, offering many properties that are more desirable. Until the 19th century, steel was only manufactured in small quantities until the invention of the Bessemer process. This process allowed for many advancements in process control, which in turn led to the mass production of steel leading it to be a vital part of the world's economy. The integrated steelmaking process is shown in Figure 1.2. Primary steelmaking involves converting liquid iron from a blast furnace through the process of basic oxygen steelmaking in order to remove excess carbon, which can be dissolved during the reduction process. Secondary steelmaking involves refining and alloying the crude steel before casting. The secondary operations are carried out in ladles and involve addition of alloying elements as well as controlling the levels of dissolved gases in the steel. Non-metallic inclusions (NMIs) are chemical compounds that are present in the steel as a result of chemical reactions and contamination that occurs during melting and pouring processes [11]. They can be further categorised as endogenous and exogenous inclusions where endogenous inclusions occur within the metal and is a result of chemical reactions and exogenous inclusions are caused by the entrapment of non-metals such as slag, fluxing residues and pieces of the mould and refractory linings [4,26]. Removing and altering inclusions chemically is also important to ensure that high quality steel is produced to meet industry specifications after casting [2,27–29]

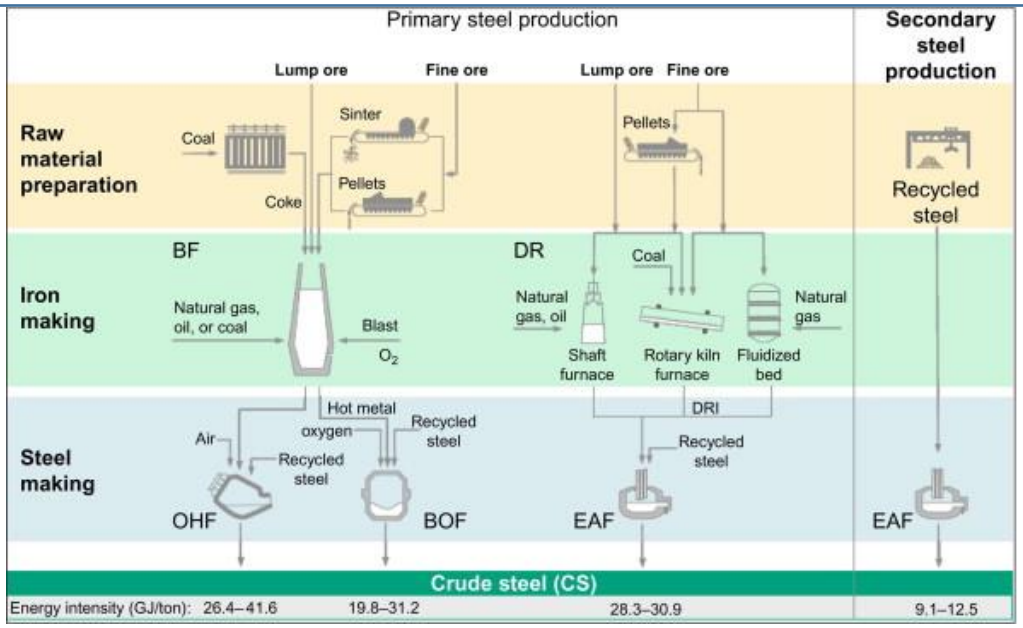

Figure 1.2 A schematic diagram showing the integrated steelmaking process with the raw material preparation, iron making and steel making with the secondary steel production using recycled steel [2]

The main routes for producing steel are through the electric arc furnace (EAF) and the blast furnace (BF). Different countries use different production routes: North America produce 60% of its steel through the EAF, whereas Europe produce 70% of its steel through the BF [30]. After molten steel is released from the basic oxygen furnace (BOF), the next step is the continuous casting or ingot casting process where the steel is formed into semi-finished shapes [31,32]. As modern steel mills requires a high throughput, the continuous casting process saves time by reducing the steps required to produce the desired shape, also reducing the need for reheating steps [33]. The steel is cooled in a continuous casting mould and put through reheating and shaping processes such as hot and cold rolling [19,31]. Most inclusions are removed in ladle processing where most primary deoxidation inclusions are formed, where the inclusions move towards the ladle slag and the ladle walls and attach themselves to it. Any inclusions remaining after this process are removed by the use of the slag layer that can entrap inclusions floating into the slag layer. The continuous caster is a critical step for controlling inclusions and removing inclusions as it is the final step where liquid steel turns to solid making it much harder to add and take components after this step.

1.3 Clean steels

Inclusions can be categorised into exogenous and endogenous depending on the reactions or processes that caused them to form [34]. Endogenous inclusions form during ladle treatment due to reactions between intentionally added alloying elements, primarily aluminium but in some cases silicon, calcium and titanium, as well as the residual oxygen from the BOF. These inclusions are a result of chemical reactions in the steel melt. Exogenous inclusions involve reactions between the melt and its environment, for example, the slag, atmosphere or refractory walls in the vessels [35]. These types of inclusions result not only from multi-phase chemical reactions but also from emulsions or erosion processes such as of the lining refractory as shown in Table 1.1. Over the last few decades, the research, development and understanding of the effects of non-metallic inclusions has caused the steel making industry to reduce the number of inclusions in the final steel product. The time and location of deoxidant and alloy additions, continuous casting practices and secondary metallurgy treatments all play a part in controlling steel cleanliness. Process control to ensure cleanliness in steel refining has become critical to continually improve the final steel product. Having a cleaner steel means to have a lower fraction of inclusions in the final product. These inclusions include oxides and sulphides [14,36]. Steel cleanliness is a relative term that can be measured on a quantitative or qualitative basis following ASTM standards such as ASTM E45 18a. Inclusions can also be more quantitatively assessed by automated SEM analysis.

Table 1.1 Origin, cause and measures to avoid inclusions for the occurrence of inclusions [7-9, 33-42]

Origin	Cause	Measures to avoid inclusions
Oxidising ladle slag	- Slag entrainment in the melt - Reoxidation of top slag and emulsified slag [7]	- Leave some steel melt in the ladle - Slag deoxidation with aluminium [37]
Reoxidation by air	- Air in tundish at transient period - Air aspiration at loose joints	- Argon injection in tundish nozzle or submerged entry nozzle (SEN) [38] - Argon seal
Tundish slag	- Slag entrainment by drainage when the bath is shallow - Slag entrainment due to turbulent melt flow at the meniscus when transferring [39]	- Large tundish with reasonable depth and residence time [7]
SEN	- Clogging by alumina leads to an asymmetric aggressive melt flow from SEN which then leads to a penetration of inclusions deep into the pool [9] - Accretions breaking into the liquid steel	- Different nozzle design such as annular or swirl [40] - Calcium addition to the melt to reduce clogging [41]
Mould slag	- Slag entrainment by turbulent metal flow at meniscus [7]	- Electromagnetic (EM) meniscus flow control [40] - Slag viscosity control [42]
Exogenous inclusions	- Large clusters of alumina inclusions forming during melt transfer into mould [40]	- Large tundish - Vertical bending caster [6] - EM damping of penetrating flow into melt pool in strand [40]

Non-metallic inclusions (NMIs) cause various defects in steel such as cracked flanges, slag spots, and line defects [4]. Reactions between inclusions and liquid steel in the continuous casting mould directly affect inclusion behaviour. Some sources of inclusions in steel are small particles of entrained mould slag or reaction products from the steelmaking processes. Mould slags are molten oxides that are used to control the lubrication and heat transfer during the continuous casting process. Removing the inclusions from liquid steel in the continuous casting process is critical to reduce steel defects and

produce high quality steels as well as preventing unwanted reactions between the steel and the mould slags to not change important properties of the mould powder such as viscosity.

Inclusions can cause defects during processing as shown in Table 1.1 or in the final product such as flange-cracked cans due to the lack of formability. The inclusions that cause these defects are calcia or alumina in composition and are around 50 to 150 microns in size. During ladle changing, continuous casting tundish slag can become mixed into the molten steel during ladle changing which is the main source of these inclusions [4]. Line defects can appear on the surface of finished strip product and it is believed to be a result of non-metallic inclusions caught near the surface of the slab [4,5].

The purpose of this research project is to investigate the reaction between high silica mould slag particles and high aluminium steel and the resulting inclusion characteristics. The reaction between inclusions (from entrained mould slag) and liquid steel in the continuous casting mould directly affects the inclusion behaviour such as their residence times and removal efficiency. However, there is a lack of kinetic information on inclusion-steel reactions, which are key to tracking the transient existence of inclusions through the steelmaking process. Inclusions (silica rich) can react with the alloying elements such as aluminium in the liquid steel melt due to there being a chemical potential for this reaction to occur. In particular the work has focussed on identifying how fast the silicon and aluminium contents will equilibrate in the inclusion and steel as a function of inclusion size and temperature, and hence the effect on inclusion residence time, related to changes in inclusion morphology and composition/density. Figure 1.3 shows the transport of inclusion particles in the continuous caster as liquid mould slag can become entrained into the flowing steel due to fluid flow problems as well as meniscus level fluctuations and excessive velocity across the slag-steel interface. Particles that reach the top layer with the mould powder are removed; otherwise, the particles are eventually trapped into the solidifying shell. Particles captured near the meniscus lead to surface defects while particles captured deep in the caster lead to internal defects in the final steel product [3]. Knowing the residence time will give an indication on how casting parameters, affecting fluid flow in the mould, will affect inclusion retention and hence how to avoid such defects and lower the number of slag inclusions in the final steel product. The knowledge created will improve prediction of inclusion residence time in the molten steel in the continuous casting process as shown in Figure 1.3 and help validate CFD models and optimise fluid flow in the mould. Ultimately, it will help produce clean steels by improving the predictability of inclusion removal from liquid steel.

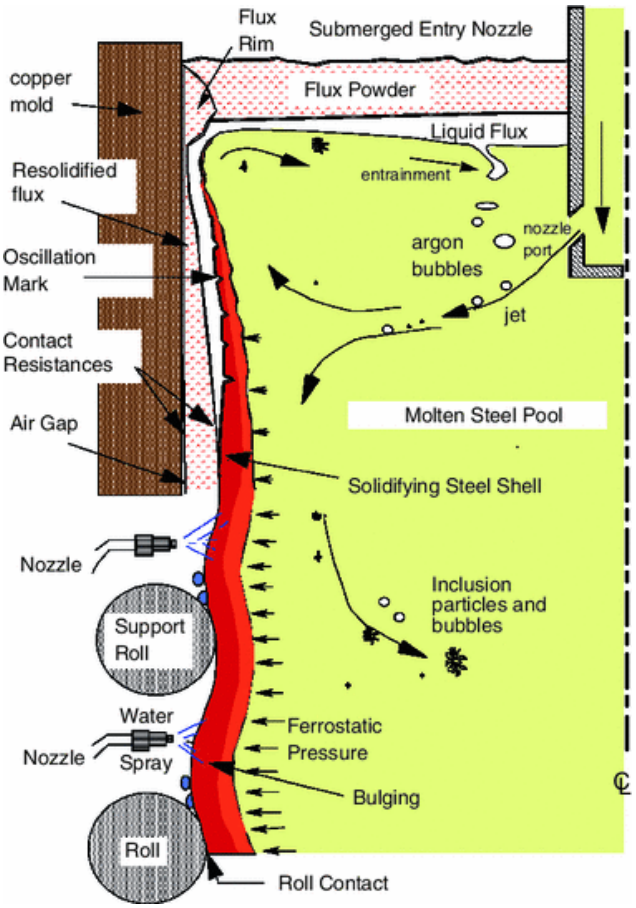

Figure 1.10 The different phenomena that occurs in the continuous casting process showing the transport of inclusion particles in the steel melt [3]

1.4 EngD portfolio structure

The structure of this report is designed to assist the reader in understanding the significance and nature of the reaction mechanisms between high-aluminium steel and high silica mould inclusions in Section 2 by reviewing the relevant literature. The methodology that has been used is discussed in Section 3. The development of the technique to investigate the reaction is explored in Section 4. Section 5 discusses the mathematical model to calculate the equilibrium compositions of the reactants and products. The experimental investigation of the reaction between an inclusion in a steel matrix, and explanation of the physical phenomena that can affect a reaction, is described in Section 6. To explore these further, experiments were undertaken at different temperatures to explore the reaction under conditions (temperatures and times) representative of those in a continuous caster as the steel is solidifying in Section 7. Section 8 discusses the applications of relevant knowledge to the steel industry and problems that are caused in the final steel product due to inclusions as seen in battery cans. Finally, the findings of the project are summarised in Section 9, highlighting the innovative novel methods applied and the potential improvements these findings can have in the steel industry. Section 10 discusses the future work where further activities are suggested that would support and extend what has been found.

To support the innovation report separate submissions have been structured as independent reports providing all the necessary information related to each section:

Submission 1 is a literature review covering the steelmaking process as well as different inclusion detection methods. This identified a need to develop a novel approach for in-situ observation of inclusions in liquid steel, which takes advantage of the advancements in high-temperature laser scanning microscopy (HT-CLSM), X-ray computed tomography (XCT) and advanced characterisation techniques. The approach offers a pathway to study the kinetics of the inclusion and steel reaction as well as producing new information on the 3D interface of the two phases during reaction.

Submission 2 titled ‘Experimental Techniques and Research Methodology’ discusses the different approaches for direct observation of the inclusion – steel reaction with the different techniques available at the University of Warwick such as HT-CLSM, high temperature furnace testing, XCT and further characterisation techniques.

The high temperature test methods used in the work are discussed in the Submission 3 such as furnace tests, pellet tests and dimple tests, all contributing to calculating the reaction kinetics between a silica based inclusion and the aluminium in the steel relevant to various points in the continuous caster (liquid inclusion—semi-liquid steel; and liquid inclusion-solid steel).

During the manufacturing of steel, a number of unwanted reactions occur at the slag-metal interface. Submission 4, titled 'Mathematical Modelling of the FeAl-SiO_2 system', focuses on the reaction between silica in the slag and aluminium in the metal. When silica is reduced in the slag, there is a transfer of silicon to the metal. The mathematical model starts with a Gibbs free energy calculation, moving on to calculation of the activity coefficients. This is used to calculate the equilibrium constant and the compositions of the components at equilibrium. Using these values, diffusion and mass transfer principles are used to calculate the kinetics of the reaction.

Submission 5, titled 'The Spontaneous Emulsification of Entrained Inclusions during Casting of High Aluminium Steels', provides experimental evidence that an entrained inclusion undergoes spontaneous emulsification when reacting with a high aluminium steel (1 wt. %). This allows the reaction rates to be calculated for a liquid inclusion reacting with liquid steel, giving information to its composition and morphology. This submission is also the accepted journal paper for Metallurgical and Materials Transactions B (2021).

The final submission is Submission 6: Reactions in the Continuous Caster, discusses the use of HT-CLSM for direct observation of the reaction at high temperature after rapid heating and control of the time-temperature of reaction, and advanced electron microscopy techniques for characterisation of the rapidly cooled samples to investigate compositional changes and hence reaction rates at different temperatures. The results for liquid inclusion – liquid steel and liquid inclusion – solid steel have been used to consider the reactions that can occur in a continuous caster as the steel cools to form slabs. This study interrogates a high aluminium steel (1 wt. %) in contact with an inclusion-slag phase with a starting composition aligned to a typical mould slag.

Submission 7: Battery cans discusses the steel defects that are found in battery cans produced by Tata Steel Europe, Ijmuiden. Line defects in the form of parabolic lines were discovered, suggesting that they may be formed due to inclusions causing these defects. Possible suggestions were given to the cause of these parabolic lines as well as SEM/EDS analysis to confirm the compositions of these inclusions that are found.

Submission 8: International Collaboration discusses the international collaborations that occurred over the course of the four-year EngD programme. As part of the EngD International programme run by the EPSRC Centre for Doctoral Training in Sustainable Materials and Manufacturing, an international placement was required. However, due to the unforeseen unfortunate events regarding the global pandemic, the international research visit was unable to be completed. It has been agreed by the EngD centre that, on an exception basis, the international collaborations throughout the EngD could be substituted for the international research visit when considering the EngD International award. As such, this document details the international collaborations throughout the EngD in chronological order.

As a result, the submissions demonstrate the different techniques used to investigate the reaction between the steel and inclusion. Table 1.2 provides a portfolio plan as a suggested reading order for the portfolio, which are referred to for further explanation or detail within this report, while Figure 1.4 demonstrates the structure of the submissions as a diagram, demonstrating the core skills required for the EngD. The findings of the submission are summarised in this innovation report as innovative application of knowledge in the steel industry.

Table 1.2 List of submissions submitted for the EngD programme

Submission Number	**Submission Name**	**Report section**
1	Literature Review	1, 2
2	Experimental Techniques and Research Methodology	3, 4
3	Artificial Inclusion Environments – Replicating Industry in the Laboratory	5
4	Mathematical Modelling of the FeAl-SiO_2 system	6
5	The Spontaneous Emulsification of Entrained Inclusions during Casting of High Aluminum Steels	7
6	Reactions in the continuous caster	5,6
7	Battery cans	8
8	International Collaboration	

Figure 1.4 Portfolio Plan and structure diagram showing submissions and published work

1.6 Research Dissemination

This work has been disseminated through journal publications, poster presentations and conferences.

Academic journal papers

- Raviraj, A., Kourra, N., Williams, M.A., Abbel, G., Davis, C., Tiekink, W., Sridhar, S., Spooner, S. The Spontaneous Emulsification of Entrained Inclusions During Casting of High Aluminum Steels. *Metallurgical and Materials Transactions B* (2021).
- Raviraj, A., Spooner, S., Li, J., Kourra, N., Warnett, J.M., Williams, M.A., Davis, C., Abbel, G., Tiekink, W., Sridhar, S. Artificial Inclusion Environments – Replicating Industry in the Laboratory. *Frontiers in Materials (2021), Accepted on 28/09/21.*

Conference poster presentations

- Raviraj, A., Kourra, N., Williams, M.A., Abbel, G., Tiekink, W., Sridhar, S., Spooner, S, Li, Z.. 'Study on inclusions causing clean steel defects', Tata Steel Theme Review, October 2017, Swansea
- Raviraj, A., Kourra, N., Williams, M.A., Abbel, G., Tiekink, W., Sridhar, S., Spooner, S, Li, Z.. 'Study on inclusions causing clean steel defects', Tata Steel Theme Review, July 2018, Swansea
- Raviraj, A., Kourra, N., Williams, M.A., Abbel, G., Tiekink, W., Sridhar, S., Spooner, S, Li, Z.. 'Study on inclusions causing clean steel defects', Tosca 2018, Warwick.
- Raviraj, A., Kourra, N., Williams, M.A., Abbel, G., Davis, C., Tiekink, W., Sridhar, S., Spooner, S. 'Blinding Ultra-High temperature reaction phenomena – unlocking the truly unseeable with XCT', 4th Annual Advances in X-Ray Imaging Workshop 2019 at Diamond Light Source, Oxford

Conference oral presentations

- Raviraj, A., Kourra, N., Williams, M.A., Abbel, G., Davis, C., Tiekink, W., Sridhar, S., Spooner, S. 'The Spontaneous Emulsification of Entrained Inclusions During Casting of High Aluminium Steels', International Student Conference in Metallic Materials, July 2020 (online)
- Raviraj, A., Kourra, N., Williams, M.A., Abbel, G., Davis, C., Tiekink, W., Sridhar, S., Spooner, S. 'The Spontaneous Emulsification of Entrained Inclusions During Casting of High Aluminium Steels', The 11th International conference on Molten Slags, Fluxes and Salts, February 2021 (online)

2. Literature Review

2.1 Where do inclusions come from?

Non-metallic inclusions originate from the reactions between reactive alloying elements in the molten steel such as aluminium, silicon, calcium and titanium, with impurities such as oxygen, nitrogen and sulphur as well as entrainment of slags and refractory materials. Oxygen primarily originates from the atmosphere, slag or reactor vessels or from the steel melt in the convertor after oxygen blowing [43,44]. Nitrogen also comes from the atmosphere and sulphur from the raw materials. In addition, inclusions can also be categorised into exogenous and endogenous depending on the reactions or processes that caused them to form [34].

Endogenous inclusions form during ladle treatment due to reactions between intentionally added alloying elements, primarily aluminium but in some cases silicon, calcium and titanium, as well as the residual oxygen from the BOF. These inclusions are a result of chemical reactions in the steel melt. Exogenous inclusions involve reactions between the melt and its environment, for example, the slag, atmosphere or refractory walls in the vessels [35]. These type of inclusions result not only from multi-phase chemical reactions but also from emulsions or erosion processes such as of the lining refractory.

2.2 Reactions between inclusions and liquid steel

Inclusions can be formed during oxidation and desulphurisation processes. The reaction between the molten metal and refractory lining of a furnace as well as oxidation by air or slags can create inclusions. Raw steel obtained from the convertor contains dissolved oxygen (200-1000 ppm). If this oxygen content is not decreased, the high oxygen content will result in a low yield of alloying additions. Due to decreasing solubility during solidification, the rejected oxygen may react with carbon and alloying elements present in the steel to form carbon monoxide and non-metallic inclusions [45]. Formation of gases like carbon monoxide can lead to problems such as blowholes and pinholes while the oxide formation results in surface or sub-surface porosity, which is detrimental for the properties of the final product. When deoxidisers such as aluminium and titanium are added to the steel melt, large numbers of primary inclusions nucleate in a very short time [46].

Modification of alumina inclusions in the steel melt by calcium treatment is a common practice that is employed prior to continuous casting of low carbon steel. Alumina inclusions formed after aluminium addition are solid particles and tend to form clusters [47]. This cluster formation can lead to blockage of the submerged entry nozzle during casting which can disrupt the entire casting operation. Addition of calcium improves the cast ability of the steel. Calcium treatment leads to the formation of calcium

aluminates which are liquid at molten steel temperature [48] and do not form clusters [49], thereby preventing the nozzle from blocking up. Addition of calcium reduces the dissolved oxygen content of liquid steel [50], therefore, more calcium can be added maintaining the liquid inclusions, thus favouring the floatation of inclusions and casting.

Calcium aluminates that have a relatively low melting point will be turned into calcium oxide, which will then simultaneously produce calcium sulphide if there are excessive amounts of calcium fed into the molten steel. This is due to calcium having a strong affinity with oxygen and sulphur. Calcium treatment can have many harmful effects on the properties and quality of the steel if it is not properly controlled. Liquid inclusions, excluding alumina, do not stick to the nozzle refractories, but if there is a high lime concentration in the inclusions, they have the potential to dissolve. As calcium has a higher affinity for oxygen compared to most metallic elements in the iron and steel making industries, calcium has the potential to reduce some parts of the refractories [49]. Calcium treatment can soften alumina inclusions but it can make clogging more of an issue [9,51]. Adding calcium is usually in the form of a silicon alloy such as CaSi with at least 30% calcium. When producing a low silicon steel, CaFe or pure Ca can be used in the form of a cored wire that is injected into the ladle. This is often done at the end of the ladle treatment when inclusions can be modified so that the inclusions become liquid at the deoxidation temperature when nozzle clogging during casting can be prevented [14,52]. To ensure good castability of the steel, the calcium content needs to be high enough to ensure that there is a complete transformation of solid alumina oxides into liquid calcium aluminates but low enough to prevent precipitation of calcium sulphides at high temperatures [14].

Another important reaction to consider in steel making is the reaction between slag reactions with alloying elements in the steel. A number of processes involve the reduction of silica in the slag and as a result, the transfer of silicon to the metal. When reacting with aluminium in the steel which is used primarily in transformation-induced plasticity (TRIP) steels [53], it can obstruct quality control as it can cause the steel to be out of specification in Si-restricted grade steels. Aluminium is added to stabilise retained austenite than transforms into martensite under strain [54]. Unwanted silicon in the metal can degrade the surface quality and coatability by forming oxides on the as-cast slab. This in turn disturbs the galvanising process and makes it difficult to use TRIP steels in commercial automobile parts. The key properties of a molten mould flux are its viscosity, crystallisation, glass formation and thermal conductivity which are highly dependent on the silicate structure, therefore the silica content [42]. A decrease in silica in the mould flux will cause problems in the continuous casting process as it can cause unwanted changes in the slag viscosity, which is critical to aid lubrication at the strand/mould interface and if there are changes in the slag crystallisation, it can cause problems for controlling heat transfer and therefore the thickness of the solid strand [53].

In the continuous casting mould, mould slag can often become entrained in the liquid steel in the continuous caster due to turbulence, steel flow, velocities and steel solidification rates. If these mould slag particles remain entrained and be trapped in the solidified steel, it can cause significant problems when producing clean steels [55]. Inclusion control in the continuous caster is extremely crucial as it is the last point the steel is liquid. Hibbeler and Thomas proposed nine possible mechanisms for the entrainment of mould slag inclusions in the continuous caster [55] including top surface fluctuations of the liquid steel pool, entrainment by bubble penetration of the slag layer (where the bubble approaching the slag layer, ruptures the slag layer causing entrainment of smaller particles in the liquid steel pool), and the possibility of the slag layer crawling down the SEN causing an issue when combined with the slag foaming with argon bubbles.

2.3 Effect of inclusions on steel products – processing and properties

Non-metallic inclusions are generally unwanted since they cause many obstacles for effective manufacturing of steel [5]. Firstly, they cause problems in the processing of steel by clogging nozzles and gates between various vessels when the molten metal is being transferred. Secondly, their presence in the final cast product is unwanted since they can degrade the mechanical properties. The specific size and shape of the inclusion particles that are harmful depends greatly on the specific thickness and application of the cast product. However, there are some extremely sensitive products such as steels for bearings or landing gears that require extreme toughness or tinplate which requires extreme processing of thin walled sections [56]. These cases allow very little tolerance for non-metallic inclusions.

2.3.1 Processing

These inclusions also cause major problems during the steel making process as it can clog the continuous casting nozzles as it causes a build-up of material in the flow between the tundish and the mould [57]. This has severe consequences as it causes a decrease in productivity, and increase in cost, as the parts need to be replaced and a decrease in quality of the final steel product. A decrease in productivity is a result of compensating for the clogging by opening the flow control device further. If the clogging becomes so severe, the flow control device cannot compensate further, and there will be a decrease in casting speed and a replacement of the nozzle as a result. This in turn reduces the casting output, reducing productivity. Depending on the type of continuous caster, certain parts of the clogged nozzle such as the submerged entry nozzle can be replaced during casting independently. Other parts such as the tundish nozzle can only be replaced by changing tundishes. Several authors have reported that nozzle clogging affects the life time of the tundish [58], for example Haers et al. [59] have found that nozzle clogging as reduced the number of heats that can be cast from twelve to six, where one heat is

290 tonnes. This shows that nozzle clogging causes additional costs for tundish maintenance as well as nozzle replacement [60].

As exogenous inclusions move due to their large size, they may entrap deoxidation inclusions such as alumina on their surface. The amount, size distribution, shape and composition of inclusions should be measured at all stages during steel production to ensure there are no abnormal clusters of inclusions which may block nozzles [57].

Steelmaking involves many different transfer operations that involve mixing of the slag and liquid metal especially when the contents are transferred between different vessels and unit operations [19,61]. This often causes slag particles to be suspended in the liquid steel with varying inclusion size from ten microns to 300 microns with large amounts of calcium oxide and magnesium oxide. During the continuous casting process, several factors can affect the slag entrainment into the molten steel. Transfer operations from the ladle to the tundish and from the tundish to the mould especially when there is open pouring of the contents. When the gas stirring is above critical gas flow rate, it can cause emulsification and slag entrainment at the top surface. Due to the high temperatures, if there is turbulence at the meniscus in the mould, which can cause the slag to become entrained in the steel. If the slag properties are also not ideal with the correct interfacial tension and slag viscosity, it can cause an emulsification of the slag in the liquid steel [38].

2.3.2 Product

Inclusions may create defects in the rolled products when they become visible at the surface of a coil or when they initiate cracks. Inclusions cause many problems when the steel is machined producing chatter, pits and gouges on the surfaces with frequent breakage as well as excessive wear and tear of the tools [62]. For automotive outer panels, tin plate and battery cans the surface of the steel is very critical and defects have an extremely low tolerance [28,63]. The total amount of inclusions must be low and large inclusions should be prevented. For example, for battery cans, which are made by deep drawing of a very thin (0.1 mm) sheet, inclusions with a size over 20 µm may already create problematic defects [64]. LCAK steel cans can suffer from cracked flanges due to lack of formability as shown in Figure 2.1 [4].

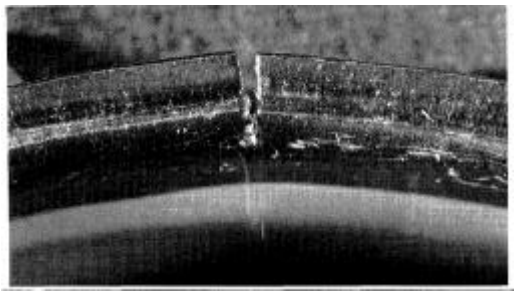

Figure 2.1 Appearance of a cracked flange can [4]

Inclusions can cause huge defects in the final steel product. These defects can be internal and external, with some external defects been seen visually as there will be a poor surface finish [65]. Inclusions can also affect mechanical properties such as ductility, fracture toughness and resistance to corrosion. These properties are not visually detected but can lead to dangerous consequences. Inclusions can be a stress raiser as it hinders the dislocation movement causing a hardening of the material. Other possible causes of defects in the final product is when particles become dislodged from the build-up in nozzles, especially in steel products that are deep drawn with a maximum inclusion size of 50 microns in diameter [66]. This can lead to restrictions in the flow and unwanted flow patterns in the mould which can lead to quality problems such as mould flux ingestion and shell thinning [67].

Non-metallic inclusions are a significant problem in cast steels that can lead to excessive casting repairs or rejected castings [68]. The mechanical behaviour of steel is controlled by various characteristics of inclusions such as its size, distribution, composition and morphology, as well as precipitates that are stress causes which can cause cracks. Large macro-inclusions are the most harmful to mechanical properties making the inclusion size and distribution important even if large inclusions are outnumbered by smaller ones [69]. The ductility of steel also reduces when there are increasing amounts of oxide or sulphide inclusions [28]. Fracture toughness also decreases when inclusions are present in higher-strength lower ductility alloys [70]. Hard and brittle oxides such as alumina particles over 30 µm [5] cause most of the fatigue problems in bearing steels.

Alumina inclusions in Low Carbon Aluminium Killed (LCAK) steel and silica inclusions in Si-killed steel are generated by the reaction between the dissolved oxygen and the added aluminium and silicon deoxidant [68]. Silica inclusions are generally spherical as shown in Figure 2.2 as they tend to be in a liquid or glassy state in the molten steel and can also agglomerate into clusters [71]. Alumina inclusions are dendritic when formed in a high oxygen environment and also form three dimensional clusters as they collide and agglomerate due to their high interfacial tension with the molten steel [72] as shown in Figure 2.3 and Figure 2.4. During cooling, the concentration of dissolved oxygen, nitrogen and sulphur in the liquid steel becomes larger as it is rejected from the solidifying phase while the solubility of those elements in the liquid also decreases, thus, inclusions such as alumina and silica precipitate [73].

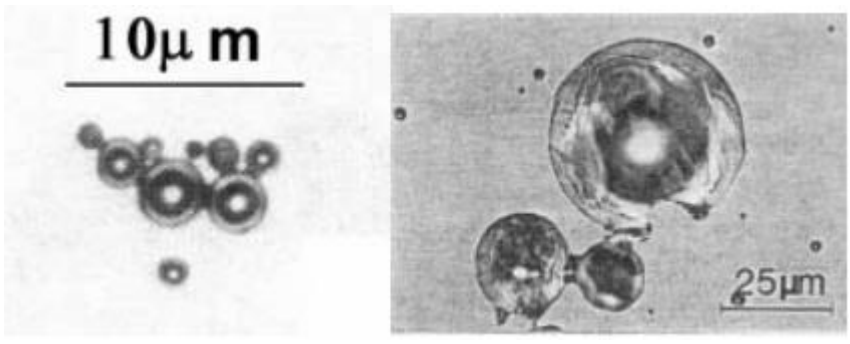

Figure 2.2 Agglomeration of round silica inclusions [5]

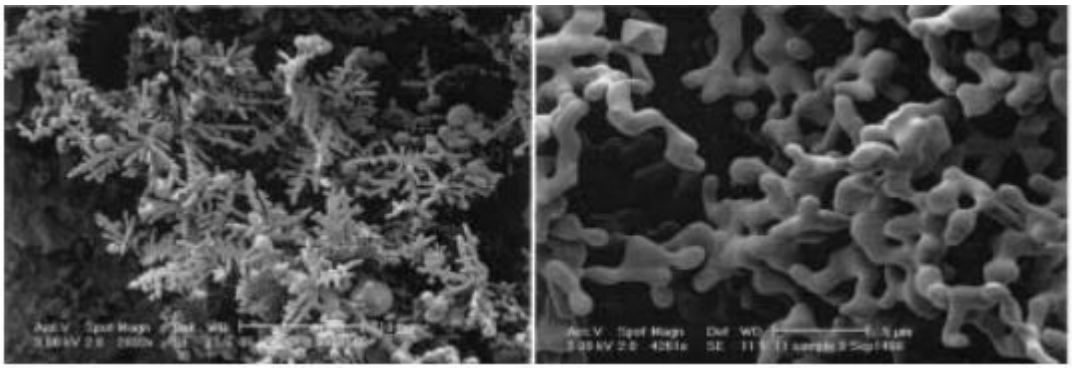

Figure 2.3 Dendritic and clusters alumina inclusions (left) and coral-like alumina inclusions (right) formed during deoxidation of pure iron [5]

Line defects, as shown in Figure 2.5, also known as slivers, plague LCAK sheet steels for automotive applications causing both cosmetic surface imperfections as well as formability problems. The three main sources for his are from iron oxide, alumina and exogenous oxide inclusions. These can be anywhere between several tens of micrometres to a millimetre in width or 0.1 – one metre in length [4,34].

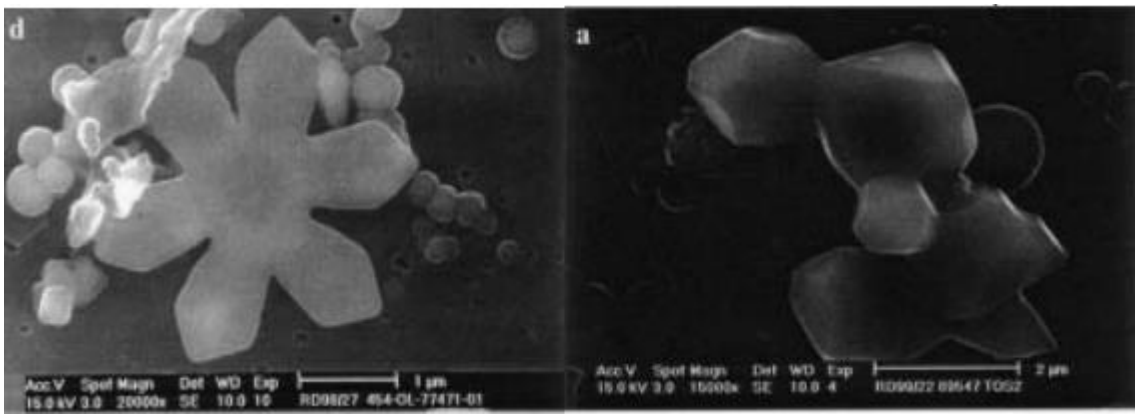

Figure 2.4 Alumina inclusions formed during the deoxidation of LCAK steel showing a flower like plate alumina on the left and aggregation of small polyhedral particles on the right [5]

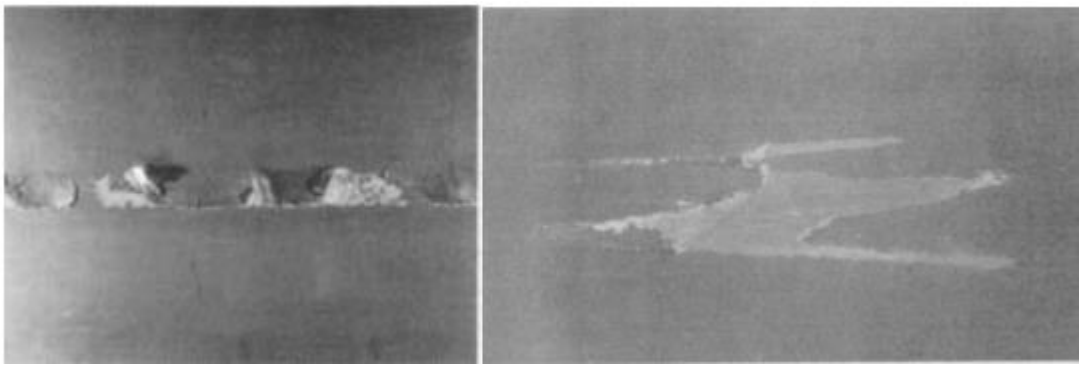

Figure 2.5 Sliver defects on the surface of sheet steel [5]

2.4 Existing evaluation techniques for inclusion detection

The characterisation of inclusions consists of evaluating its size, distribution, morphology and chemical composition to determine the type of inclusion [74]. There are a variety of techniques that can be used to determine the inclusion content of the steel industrially, however, the size, and time needed for inspection as well as the volume of the material needs to be taken into consideration. There are a variety of methods available to detect inclusions in volumes of solid steel as well as sections of solid and liquid steel [4]. Conventional methods such as optical microscopy to ultra sound testing, optical emission spectroscopy, laser induced spectrometry, XCT, and automated SEM are often used to detect inclusions[4]. Scanning electron microscopy with energy-dispersive X-ray spectrometry can give chemical analysis and metallographic images [11]. More modern equipment in the form of an automated system allows the entire sample to be scanned. Indirect methods are also widely adopted in industry to determine the number of inclusions and consist of determining the chemical composition of the slag as well as the conditions of the refractory and even elements that have dissolved in the bath. The total oxygen content of the steel samples can directly relate to the presence of inclusions [10]. The equipment used for this method can also measure the dissolved nitrogen in the sample, which can then be used to analyse the nitrogen pick up [8]. This can also be used to give a good indication of air absorption by the bath which is directly related to reoxidation. Table 2.1 summarises the type of sample required for different analysis and characterisation techniques.

Table 2.1 The most common sample types and the different characterisation techniques that can be used, both direct and indirect methods to analyse inclusions [4,8–15,75].

Type of sample	Analysis	Characterisation techniques
Immersion samples of steel	• Chemical composition of steel • Inclusion analysis • Total oxygen content	• Optical emission spectroscopy (OES • Pulse discrimination analysis (PDA) • Oxygen analyser SEM/EDS
Pin steel	• Chemical compositions of steel to show carbon and sulphur content	• Optical emission spectroscopy (OES

	• Inclusion analysis • Total oxygen content	• Pulse discrimination analysis (PDA) • Oxygen analyser SEM/EDS
Bar or plate steel	• Chemical composition of steel • Inclusion analysis • Total oxygen content	• Optical emission spectroscopy (OES • Pulse discrimination analysis (PDA) • Oxygen analyser SEM/EDS
Slag	• Chemical composition of the slag	• X-ray fluorescence
Clogging mass	• Chemical composition • morphology of inclusions	• SEM/EDS

A widely used technique to measure steel cleanliness is through the use of an automated SEM which is also equipped with an EDS probe [13,14,44,76]. The EDS probe allows for the composition of inclusions to also be found as well as identifying the position and morphology [76]. Using an automated SEM allows for all the particles to be scanned in the sample and collating all the data. Using manual methods does not allow for all the inclusions to be analysed, only those that are detected by the user. Capabilities of the SEM machine is also important as that will dictate the time taken for analysis as well as how much automation can be applied as well as the sample size/area.

Total oxygen content is often used as the measurements are quick and the samples can be easily obtained [8–10], but it only provides information on oxide inclusions, not any other inclusions that may be present. In combination with SEM/EDS, exact compositional data can be identified, giving information on whether the inclusions are alumina, silica or calcia, as well as giving information on the morphology. There is an efficient correlation with process data as they do represent the micro inclusion population [9,10]. Several methods can directly measure inclusions in the three-dimensional steel matrix. Using ultrasound or x-rays can scan through the sample or other techniques can be used to separate the inclusion from the steel [38]. Conventional ultrasonic scanning uses a transducer to emit sound pressure waves that is transferred into the sample with the help of a coupling gel [77,78]. An oscilloscope is used to compare the signals emitted to then indicate the quality of the sample. This non-destructive test method can be used to detect inclusions larger than 20 microns in solidified steel samples [5]. X-rays can also be used as a non-destructive test method that uses the variation of x-rays attenuated through the solid steel to image inclusions as they have a different density [79]. Destructive methods such as chemical dissolution are also used using acids to dissolve the steel and extract the inclusion [4]. Further characterisation can be done using SEM/EDS to study the morphology and composition, revealing the three-dimensional nature of inclusions. The disadvantage of this technique is that the

acid will dissolve any FeO, MnO, CaO and MgO in the inclusion so it can be used to detect and analyse Al_2O_3 and SiO_2 [5]. Electrolysis can be used for relatively large samples of steel of up to 2 kilograms by immersing it in a solution of iron chloride or iron sulphate to reveal individual and intact inclusions, however this can break up inclusion clusters into smaller particles [9]. 2.4 Conclusions

Over the last fifty years, the understanding of the effects of non-metallic inclusions in steel properties has caused the steel making process to evolve from preventing the inevitable contamination to optimising inclusion composition, amount and distribution to cause the least possible effect and damage. This has affected all the steps in steel manufacturing including the raw material selection, slag composition, optimisation of the secondary refining conditions such as the time taken to process, the rigorous control of the tundish and mould operations and the strict controls to reduce oxidation has now become a standard in quality steelmaking.

The detection methods used study the surface of the inclusions on the steel surface, which involves some destruction of the sample. Therefore, the reactions and interactions of inclusions with liquid steel have not been able to study the interactions of an inclusion wholly enclosed in the liquid steel and its 3D nature. Therefore, a combination of techniques has to be used to study the kinetics of the inclusion and steel reaction as well as producing new information on the 3D interface of the two phases during the reaction.

As non-metallic mould slag inclusions are detrimental to nearly all grades of steel, which can result in losses of yield, the findings from this research offers relevant extended insight to the wider steel grade production landscape. Steel manufacturing is an extremely energy intrusive process that also has a high carbon footprint, as such improving any aspect of the yield would have an enormous effect on sustainability due to the large tonnage of steel produced worldwide. The steels used in this study are representative of AHSS (Advanced High Strength Steel) including TRIP (Trans- formation Induced Plasticity) steel and DP (Dual Phase) steel, which have gained widespread attention for their low cost, high strength and reasonable ductility, giving timely pertinence to study the inclusion-steel behaviors for these systems.

3. Research Approach

Over the last few decades, the research, development and understanding of the effects of NMIs has allowed the steelmaking industry to reduce the number of inclusions in the final steel product [80]. The understanding of the steel and slag compositions as well as the processing conditions has dramatically improved [12,42].

By taking into account the gaps in the literature, it is clear that the methods that are currently being used to study inclusions have not been able to monitor inclusion reactions within the steel matrix [43]. With this knowledge and considering the industrially aligned deliveries and intended use of finding from this project, several hypotheses are considered using a combination of techniques available including high-temperature confocal laser scanning microscopy (HT-CLSM), X-ray computed tomography (XCT) and post-mortem electron microscopy techniques.

3.1 Research Questions to be explored

3.1.1 Hypothesis 1

'The interaction between steel and an inclusion can be studied using a combination of high-temperature confocal scanning-laser microscopy (HT-CLSM) and X-ray computed tomography (XCT)'

The gaps in the literature have shown that the interaction between steel and an inclusion needs to be investigated without destroying the sample so that the inclusion behaviour can be studied whilst being surrounded by the steel matrix as it is 3D in nature. Based on this, a novel approach between HT-CLSM and XCT as well as using SEM/EDS will be developed to study inclusions within the steel matrix without dissolving the steel. This will allow the morphology of the inclusion to be studied before destroying the sample to study the composition. An experiment using slag droplets in steel using the HT-CLSM to melt the samples and further imaged using an XCT scanner will allow the inclusion to be detected within the steel matrix. The inclusion analysis will be completed using scanning electron microscopy with electron dispersive spectroscopy (SEM-EDS) to gain compositional analysis to study the reaction.

3.1.2 Hypothesis 2

'The floatation times of inclusions will be influenced by the exchange of material across the inclusion-steel interface which is driven by the systems starting chemical potential.'

Inclusions causing clean steel defects often consist of small particles of reacted mould slag, which are molten oxides that are used to control the lubrication and heat transfer in the continuous casting process [20,81]. Kinetic information of the reaction between the inclusion and steel, and any consequent change in the inclusion morphology and/or composition, will allow the residence time of the inclusion to be calculated in liquid steel. The same techniques will be used as Hypothesis 1. Using SEM-EDS, the chemical exchange between the inclusion and the steel can be studied to give further knowledge into the reaction kinetics. This will also give experimental data that can be compared to the mathematical model for the reaction. Further equilibrium tests will be carried out using the High Temperature Bottom Loading Furnace to validate the mathematical model. To develop this further and to consider the other reactions that occur in the continuous caster, an inclusion will be placed in an indent on a steel cube and heated at two temperatures to study the reactions rates while the steel is solidifying.

3.1.3 Hypothesis 3

'Interfacial tensions between the steel and the slag can slow down the floatation of the inclusion.'

Inclusion removal follows the pathway of travelling from the liquid steel then through the slag/metal interface then into the bulk slag phase [82]. There are many interfacial forces that will play a considerable role that could affect the floatation time of the inclusion through liquid steel. A meniscus is expected to form as shown in Figure 3.1 due to the interfacial tension forces that can balance at the steel/slag/inclusion interface which can slow down the inclusion that is trying to pass through into the slag layer. Stokes' Law can be used to calculate the floatation of the inclusion but it is a simple calculation only taking into account density, dynamic viscosity and the size of the inclusion when other factors that can affect the floatation include, but are not limited to, the compositional change as well as a change in state which can in turn affect the density. The composition of the inclusion may change if there is a reaction that occurs which can then affect the viscosity. Size of the inclusion can also change if the inclusion breaks apart of if any bubbles are present. Other factors that need to be considered are the steel velocity in the continuous caster, and other physical phenomena such as film drainage and spontaneous emulsification, phenomena heavily influenced by changes in interfacial tension [83–85].

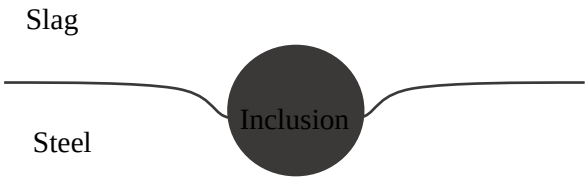

Figure 3.9 Schematic diagram showing the inclusion approaching the steel/slag interface

3.1.4 Hypothesis 4

'The nano-scale structure of alumina inclusion surfaces in a steel defect after rolling may indicate the presence of a gas phase in the slab.'

Tata Steel Europe, Ijmuiden, have observed that alumina particles near gas bubbles on a nano-metre scale have showed terraced shaped structures which could be explained by the Burton-Cabrera-Frank mechanism, which is based on the presence of defects on the crystal surface. The Burton-Cabrera-Frank mechanism states that terraced shaped surfaces can form due to transport and growth processes when minimising crystal surface energy in a process known as surface roughening These structures grow at low driving forces and have low growth rates [86] and this terraced shape structure is shown in Figure 3.10 [87]. Due to the presence of a gas phase, the mass transfer could be limited causing a slow crystal growth resulting in the terraced shapes. To begin this study, alumina defects in steel will have to be investigated to see if gas bubbles were involved. This may help to understand the formation of the parabolic defect lines observed in battery cans and certain defects in automotive sheet steel which are known to be influenced by alumina inclusions as alumina does not deform under the pressures of rolling. Battery can samples will be inspected visually as well as using electron microscopy.

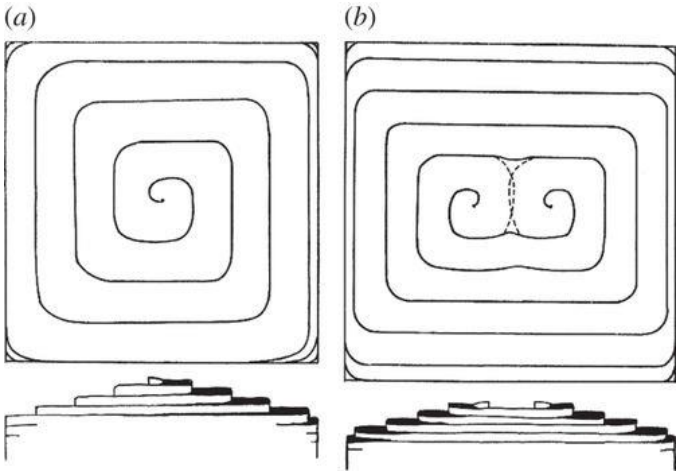

Figure 3.10 Schematic of terraced shaped structures formed by the Burton-Cabrera-Frank mechanism [87]

4. Experimental Methods

4.1 High-Temperature Confocal Laser Scanning Microscope (HT-CLSM)

The HT-CLSM is a fundamental tool for this research as it offers several advantages over conventional light optical microscopy including the ability to control depth of field, elimination or reduction of background information away from the focal plane and the capability to collect serial optical sections and three-dimensional imaging from thick specimens [88,89]. Several other researchers have used this equipment with great success to study the interaction of Fe-Al droplets with $CaO\text{-}SiO_2\text{-}Al_2O_3$ slags [90–93].

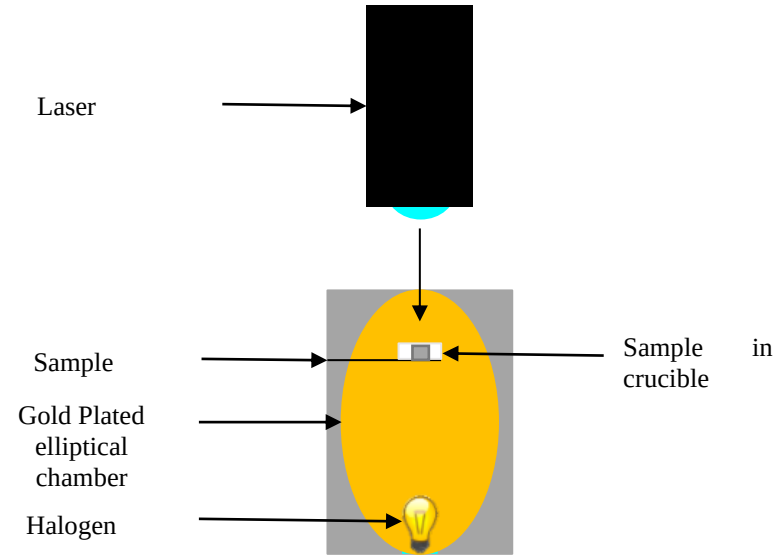

Figure 4.1 Schematic of the HT-CLSM, showing the different components of the equipment.

The equipment has an elliptical gold-coated chamber with a halogen bulb in the lower focal point of the chamber with the sample placed on the stage (made of a platinum ring with an R-type thermocouple supported by an alumina rod from the side of the chamber [84]) in the upper focal point as shown in Figure 4.1. The combination of the use of small samples in the HT-CLSM and rapid radiation output from the halogen bulb allows for heating rates of up to 973 K a minute to a maximum temperature of 1973 K. The bulb irradiates infrared light which is reflected off the gold chamber and focusses on the sample, in turn heating the sample. As the experiments are highly reactive, the chamber is kept at a positive argon pressure. HITOS is the software package that is used to control the furnace and LM-Eye is used to control the video function of the equipment. A UV laser is used to image the surface of the sample

to avoid noise from the IR-radiation emitted from the bulb and the hot sample. This equipment is fitted with a rotary vacuum pump and a high purity argon gas feed supply which is passed through a further circuit of getters, filters, drying chambers, and a heated getter at 623 K containing copper and magnesium turnings. This results in an oxygen level of less than two parts per billion which has been confirmed using gas mass spectrometry.

4.2 X-ray Computed Tomography (XCT)

X-ray computed tomography, often abbreviated to XCT is a method that uses X-ray radiation to take a number of two dimension (2D) images of an object in many positions around an axis of rotation. These 2D images are then reconstructed to produce a full 3D visualisation. These scanners are used for industrial non-destructive testing due to the increase in resolution that is available when compared to medical XCT scanners. XCT therefore provides the ability to detect small defects compared to traditional radiography [94].

The Zeiss Versa 520d X-Ray CT scanner is capable of scanning samples less than 90mm in size with a voxel resolution ranging from 25 micron to 170 nm which is dependent on the size of the sample (smaller the sample, better the resolution). The maximum voltage of the x-ray source is 160kV. Another XCT scanner that has been used is the Nikon XT H 225/320 LC. This industrial XCT scanner uses X-ray equipment to produce highly detailed three dimensional images of the sample. The results can also be flaw detection and porosity calculations. It consists of an X-ray micro-focus source of 225kV or 320 kV with a choice of molybdenum or tungsten target. The detector panel consists of 2000 pixels of 200 micron in size. The achievable resolution is 5– 170 micron voxel resolution with a maximum object diameter of 280 mm and a maximum object height of 600 mm.

4.3 Sample Preparation for SEM

To prepare the samples for SEM analysis, the samples need to be mounted using EpoThin™ 2 Epoxy Resin and EpoThin™ 2 Hardener in a two to one ratio. This resin is suitable for the steel samples as it produces a clear, bubble free mount which offers an unobstructed view of the embedded samples. As the samples may have pores and can be heat sensitive, this epoxy is suitable as it cures at 300 K with best results after 24 hours of curing. Once the samples have cured, the samples are taken out of the mould and polished using a Buehler AutoMet™ 250 Pro Grinder-Polisher.

4.4 Scanning Electron Microscopy (SEM)

Electrons can be used as an electromagnetic radiation source instead of light. Electrons are emitted from an electron source, which is typically a tungsten filament or a field emission gun (FEG) with a voltage

ranging from 1 – 20 keV. This electron beam is condensed to a specific point of 0.5 – 5 nm by condensing lenses in the gun column which is then rastered onto the sample. Using an electron source allows a greater resolution of around a nanometre which is not quite small enough for atomic imaging. This beam of electrons interacts with the sample to product secondary electrons, backscattered electrons and electromagnetic radiation. Secondary electrons are the primary source for imaging which are formed when the electron beam interacts with the sample which causes loosely bound electrons to ionise. Backscattered electrons are the result of the elastic collisions between incoming electron beam and the sample. The resolution of the images produced through backscatter electron is around a micron due to the high energy elastic collisions causing there to be an interaction depth of approximately a micron [95].

The Zeiss Supra 55VP SEM and the Joel 7800 F-SEM can be used to study the microscale structures of materials which in combination with Energy Dispersive X-ray Spectroscopy (EDS) to study the chemical compositions of the material and Electron Backscatter Diffraction (EBSD) to analyse the texture and crystallographic orientation of each grain within the sample. In situ testing is also possible with these systems either by applying a high temperature or a mechanical stage. The Zeiss Supra 55VP SEM is used with an accelerating voltage between 1-20kV. It is fitted with a FEG source and an EDAX Genesis analysis system. If a material is non-conducting, the material will suffer from charging effects. This will cause a build-up and an uncontrolled discharge of electrons from the sample leading to an extremely distorted image. To counter this, the sample is carbon or gold coated and a silver dag is applied to the edge of the sample. The samples were scanned using a 160kV source with an exposure time of 13 seconds and a magnification of x0.4. The resultant voxel size is 27 microns with 3235 projections.

4.5 High Temperature Bottom Loading Furnace

The bottom loading furnace uses an electrically operated elevator hearth which rises into the furnace chamber and lifts the load into the heated zone and can be flushed with argon to keep it in an argon atmosphere. The furnace provides many advantages as it allows for easy loading of the samples and uniform heating is achieved as it has heating elements in all the side walls and has capabilities of reaching 1873 K. A heating rate of 283 K per minute was used and a cooling rate of 283 K per minute was used to ensure the crucible did not crack due to thermal shock.

4.6 Experimental Materials

The materials listed below were provided by Tata Steel Europe, Ijmuiden for the purpose of this study.

4.6.1 Bulk metal alloys

Bulk metal alloys were produced at Tata Steel Europe, Ijmuiden with concentrations of 0.04 wt% and 1 wt% aluminium. The 0.04 wt. % Al steel is a piece from slab material from the production plant and the 1%Al is from casts made at Tata Steel Europe laboratory vacuum induction melting facilities in 25kg ingots as shown in Table 4.1.

Table 4.1 Composition of iron alloys measured using Spark OES, all wt%

Element	Fe	C	Si	Al	O	Mn	S	P	Ni	Cu	Cr
Low Al Steel	99.7600	0.1974	0.0020	0.0400	0.0006	-	-	-	-	-	-
High Al Steel	98.800	0.1974	0.0020	1.0000	0.0006	-	-	-	-	-	-

4.6.2 Iron powder

The iron powder, used in pellet testing, was purchased from BASF, named as low carbon carbonyl iron powder (CIP CC). The composition of the iron powder as provided is shown in Table 4.2.

Table 4.2 Composition of the iron powder as provided by BASF measured using ICP, all wt. %.

Element	Fe	C	Mn	Si	S	P	Ni	Cu	Cr
Wt%	99.9968	0.0004	0.0001	0.0001	0.001	0.0008	0.0002	0.0001	0.0002

4.6.3 Bulk slag/mould powder

The mould powder 450SD was purchased from Vesuvius. Tata Steel Europe then decarburise the granulated powder and melt it. After melting, it is broken into smaller pieces and sieved to give 350 - 450 micron spheres. The composition is shown in Table 4.3.

Table 4.3 Composition of mould slag powder was measured using ICP, all wt%.

Compound	Na_2O	MgO	Al_2O_3	SiO_2	SO_3	K_2O	CaO	MnO	FeO	F
	3.5	1.1	7.4	42.2	0.3	0.1	41.6	0.2	0.5	3.3

4.6.4 Crucibles

Several crucibles were used for these experimental tests.

- For the HT-CLSM tests, alumina crucibles from AdValue Technology with diameter of 8 mm, height 4.5 mm, and thickness 0.5 mm.
- For the furnace tests, three different crucibles were used:
    - Alumina crucibles from Almath Crucibles Ltd made in recrystallized Alumina (99.8 %) with a maximum working temperature of 1750 °C
        - Size: 3.7 ml capacity, diameter of 19 mm, height of 20 mm
    - Zirconia crucibles from Almath Crucibles Ltd made in Yttria Stabilised Zirconia with a maximum working temperature of 2250 °C
        - Size: 8.6 ml capacity, diameter of 22.5 mm, height of 33 mm
    - Magnesia crucibles from Tateho Ozark made from high density magnesia with a maximum working temperature of 2852 °C
        - Size: 3.17 ml capacity, diameter 31 mm, height 76 mm

4.7 Conclusion

Having considered the various techniques that can be used to study the interactions of inclusions within the steel matrix, a combination offers unique advantages. HT-CLSM offers high temperature testing that is quick and XCT for materials science is a novel approach that can be used to locate the inclusion using a non-destructive approach. This also speeds the process of locating the inclusion as the exact location of the area of interest is known before sectioning, polishing and grinding. Advanced characterisation techniques can be used to study the inclusion and steel reactions including the element exchange between the steel and the inclusion, further proving mathematical kinetic models. The ability to employ correlative investigation across all these different experimental techniques forming a bridge between high temperature testing, metrology, and characterisation offers the potential to break new ground in an innovative way to understand inclusion behaviour in a highly unpredictable, chemically unstable system.

5. Artificial Inclusion Environments – Replicating Industry in the Laboratory

The gaps in the literature have shown that the methods that are used to study inclusions and their reactions and interactions with liquid steel have not been able to study the interactions of an inclusion wholly enclosed in the liquid steel, and its 3D nature[9]. In order to understand the reaction between slag inclusions and liquid steel that can occur in the continuous caster laboratory experiments need to be defined to reproduce the key conditions of the steel being in contact with an inclusion with the same compositions as the mould powder as well as the temperatures that these reactions happen at. Using a combination of techniques starting with artificial sample preparation (ensuring that the composition, size and morphology of both the inclusion and the steel are known), melting these samples in the HT-CLSM, then XCT can locate the position and morphology of the inclusion, which can accurately prepare the samples for post-mortem SEM/EDS analysis. As these samples will replicate industrial environments, the artificial samples will ensure a level of accuracy as the starting conditions are known.

Floatation times can be calculated, based on the quantified inclusion characteristics, as they can be influenced by the exchange of material across the steel-inclusion interface which is driven by the chemical potential. Flotation rates are important as they can be used to calculate the residence time of a reacting inclusion within the continuous caster. The chemical exchange can also give further knowledge into the reaction kinetics which can give experimental data to validate the mathematical model for the reaction. The systems under investigation are 0.04 wt. % and 1 wt. % aluminium steel with a silica rich mould slag powder that has also been made into artificial inclusions.

5.5 Powder press samples

The powder press samples were the first iteration of artificially placing an inclusion inside a steel matrix. These samples were produced using sintered steel which could be melted using the HT-CLSM then XCT scanned and analysed using Avizo. Further information can be found in Submission 3: Artificial Inclusion Environments – Replicating Industry in the Laboratory. To make a sintered steel sample, Fe powder is mixed with a binder and pressed into a layer at 1 MPa. This step is repeated until the desired sample is produced. The completed sample is pressed at a pressure of 20 MPa. An inclusion can be placed between the layers and the sample is then sintered in a furnace. The steel is then placed on a zirconia sheet and placed in a furnace heating at a rate of 393 K – 413 K per hour and a dwell of 2 hours

at 1573 K in a hydrogen atmosphere. The Zeiss Versa 520d X-Ray CT scanner was used for these tests. An XCT image of a powder press sample before melting is shown in Figure 5.1 showing the position of the inclusion within the steel sample.

As Figure 5.1 shows the position of the inclusion is not in the centre of the sample meaning that the sample needed to be scanned before and after melting to identify the starting location, size and morphology of the inclusion as every sample was not uniform. As a high-resolution scan takes 26 hours, each sample would take around four days to analyse / test / analyse. The porosity also poses a problem for the test as it is an added uncertainty that could affect the morphology and reaction of the inclusion with the steel. Any pockets of air can cause the inclusion to float quicker in a steel sample by forming a bubble and attaching to the inclusion [34,96]. A more reliable test method was needed to ensure that the position of the inclusion and the consistency of the steel was consistent.

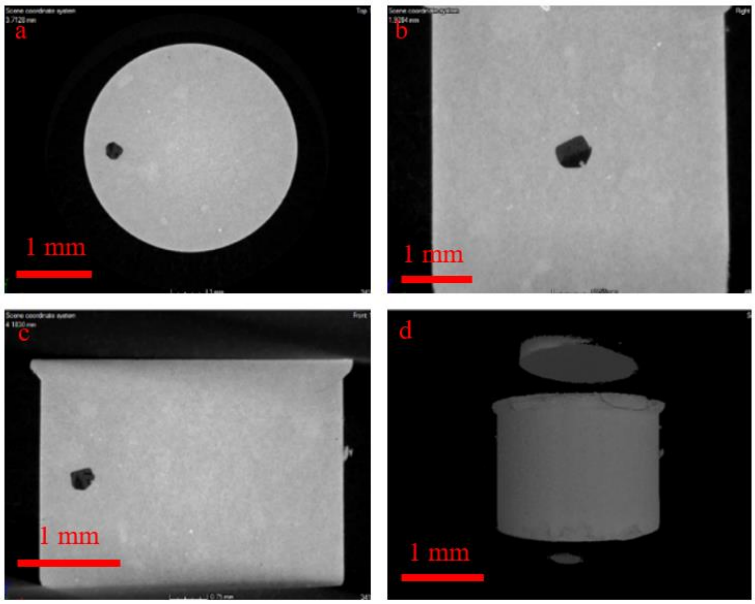

Figure 5.5.1 An XCT image of a powder press sample before CLSM melting: a) top view of the sample showing the position of the inclusion, b) side view of the sample showing the position of the inclusion, c) another side view of the sample showing the position of the inclusion using the VGSTUDIO MAX software.

5.6 Pellet samples

Using the findings of the powder press samples, it was decided that a sample is needed with very little porosity. The pellet samples are machined by electrical discharge machining (EDM). The pellet samples are small cylinders of steel that have a hole drilled into the top surface. A mould slag particle is placed into the drilled hole which is then filled with iron powder. A steel stopper was used to press the hole closed. These samples were made in two sizes: 3mm diameter, 4mm height and 5mm diameter, 6mm height. A XCT 3D image is shown below in Figure 5.2.

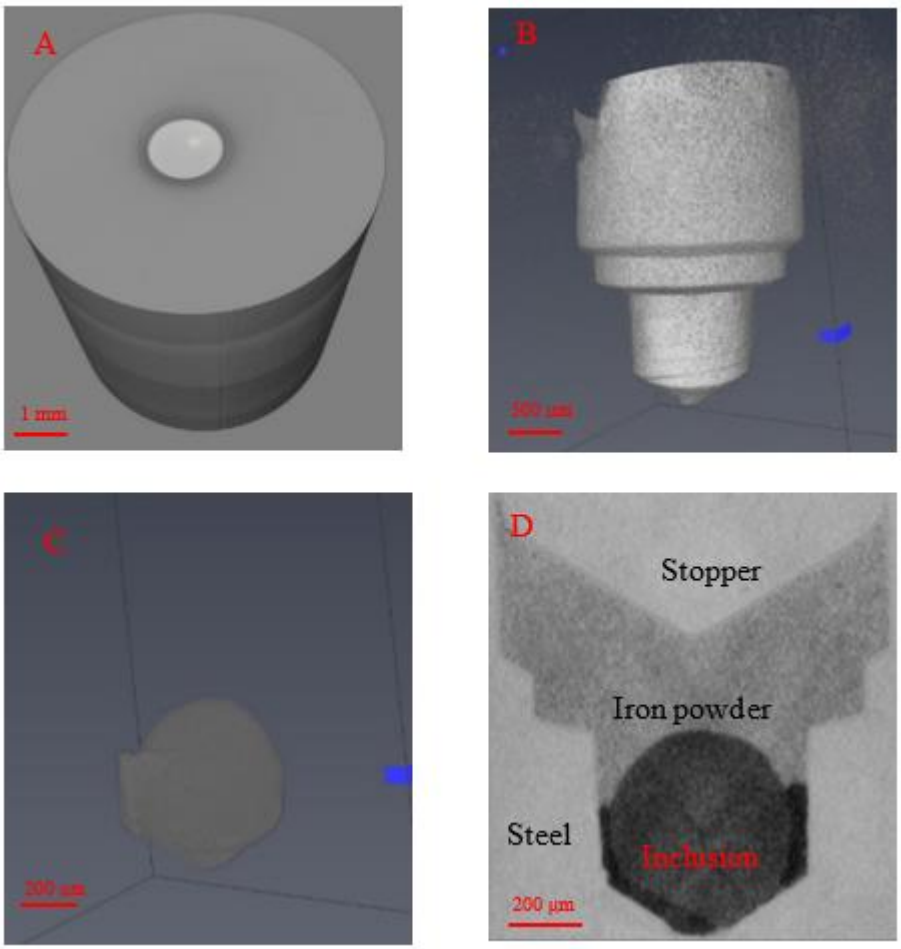

Figure 5.5.21 XCT scans of samples. a) Whole pellet, stopper can be seen. b) Removing the steel matrix, the stopper with the inclusion and iron powder. c) Inclusion and iron powder with the inclusion being the round part. d) Ortho slice of sample.

Two different heating regimes were used to test the pellet samples in order to study the liquid-liquid interactions of the steel and the inclusion. A slow heating regime was designed to minimise overheating and keeping the viscosity of the steel high. The sample was held at 1550 ℃ for five to ten minutes. The fast heating regime was designed to allow for a time resolution for the reaction as both the inclusion and the steel will be molten at the same time. At the highest temperature of 1600 ℃, the sample was held for a maximum of twenty seconds and quenched quickly.

With the slow heating regime, the steel sample did not melt completely as shown in Figure 5.3 as there is still evidence of the steel stopper. The middle of the sample does appear to have melted as the inclusion has broken apart with evidence of large amounts of porosity as well. The slow heating regime is not suitable to obtain a kinetic study as there is no time resolution as the inclusion and steel become molten at different times so the inclusion has already started reacting so it does not fulfil one of the main objectives of the project. However, XCT scans of samples melted using the fast heating regime

shows a fully melted steel sample (no indication of the steel stopper) with the inclusion embedded as shown in Figure 5.4.

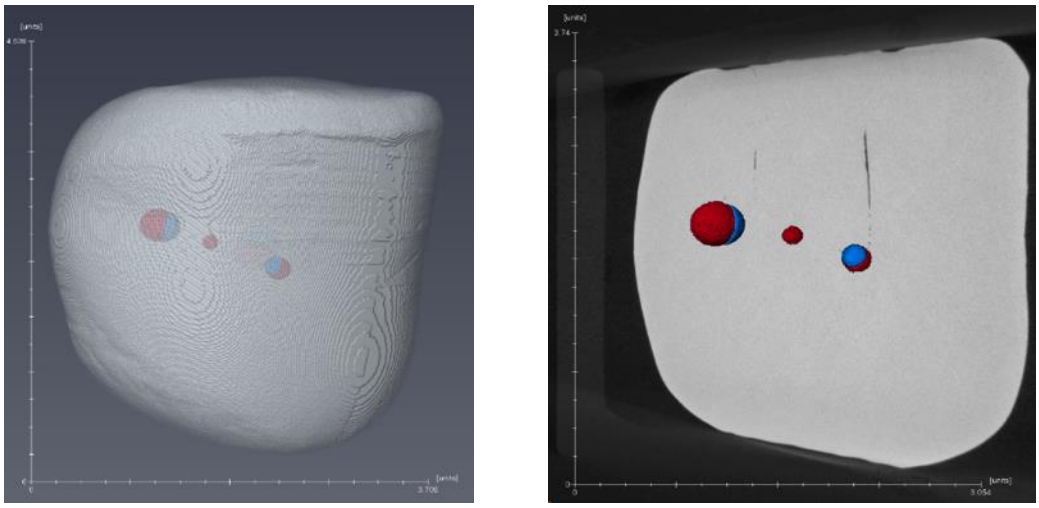

Figure 5.3 Showing a sample melted with the slow heating regime where the blue is porosity and red is inclusion

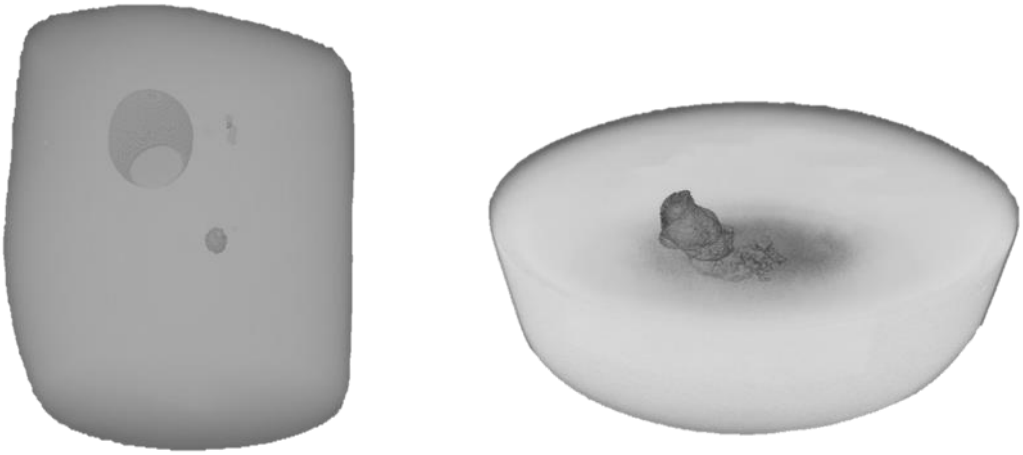

Figure 5.4 Two 3D XCT scans of a fast heated sample showing the inclusion within the steel matrix showing the inclusions

For the slow heating regime, it was difficult to ensure whether the steel (liquidus temperature of 1783 K for the 1 wt. % Al steel was used as a reference) had melted completely or not. It did mean that the inclusion did remain in the steel sample and the risk of it floating out was minimised, however a time resolution for the reaction was difficult to be determined as it was unknown when the steel melted. This is an advantage of the fast heating regime. As the sample was quickly heated to 1600℃, a time resolution could be calculated as it was visible through the HT-CLSM's UV laser when the steel had melted. A

disadvantage of the fast heating regime was that the inclusion has a tendency to float out of the steel sample so the experiment could not be held for longer than 20 seconds. This experimental method also had a very low success rate (15 samples were tested) but if samples were successful, reaction kinetics could be calculated. Results of this experimental technique are discussed in Section 7.

5.7 Dimple tests

In the continuous caster, there are many different reactions that can occur between the steel and inclusion related to whether the conditions are liquid inclusion – liquid steel; liquid inclusion-solid steel; solid inclusion-solid steel. This test method aims to explore these reactions and the resulting compositional changes at different temperatures, and therefore different states. The 1 wt. % aluminium steel was cut into 0.5 cm edge length cubes using EDM and a pilot drill was used to indent the sample to a depth of 0.5 mm with a diameter of 0.5 mm for the placement of a larger inclusion of size 600 microns on the surface in Figure 5.5

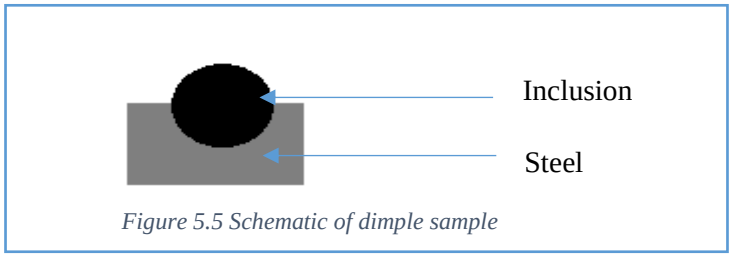

Figure 5.5 Schematic of dimple sample

The sample was placed into an alumina crucible and loaded into the HT-CLSM. Samples were tested at two different temperatures: 1473 K and 1873K (liquid inclusion-solid steel and liquid inclusion-semi-solid steel, respectively) and held for time of up to 30 minutes and 20 seconds, respectively. Melting the steel around the inclusion is quite difficult as there is a small window of 20 seconds before the steel melts completely so the higher temperature tests can only be held for 20 seconds otherwise the inclusion and steel completely melts and the position of the inclusion is lost.

5.5 Furnace Tests

This test and sample were designed using a large crucible with a cube of steel of varying compositions covered with mould powder supplied by Tata Steel Europe as shown in Figure 5.6. Several crucibles have been used for this experiment including alumina, zirconia and magnesia as the reaction between the molten slags can often react with the crucible material so several options had to be tested. The aim was to investigate the equilibrium reaction products from the steel-mould powder reaction to verify the mathematical model developed to calculate the equilibrium compositions of an aluminium steel and a reacting mould slag inclusion.

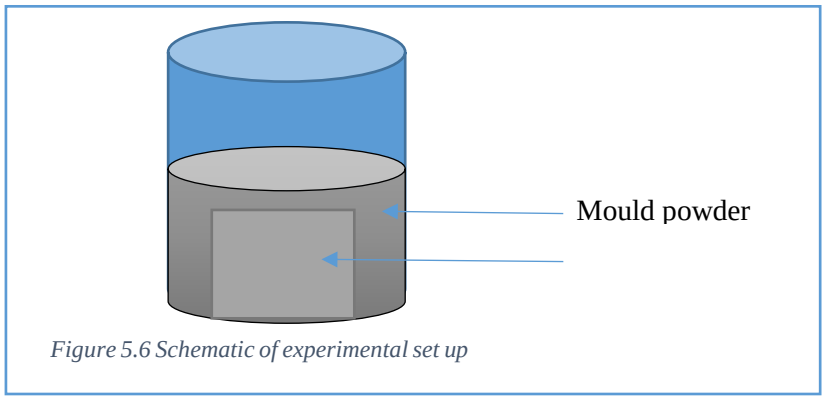

Figure 5.6 Schematic of experimental set up

5.6 Comparison of Techniques Summary

The various test methods discussed have allow detailed investigation into the reaction between a high aluminium steel and an inclusion with the chemical any physical changes and their implications discussed elsewhere in the literature [97]. Each test method has its own advantages and disadvantages as shown in Table V1 and summarised below.

The powder press samples showed the ability to embed an inclusion and the capabilities of using sintered steel to create a sample for this study. The powder press pellets are not appropriate for this study due to influence of porosity on the inclusion morphological changes during heating when the inclusion becomes molten, and the location of the inclusion to begin with, however could be important for studies relevant to other processes such as powder 3D printing.

The pellets with an inclusion are suitable to replicate industrial conditions as close as possible with an inclusion completely surrounded by molten steel. The pellet samples were useful when studying the reaction between the matrix and an entrained particle giving valuable information about the morphology changes of the inclusion as well as chemical compositions of the inclusion and surrounding steel. The limitation is the length of time the high temperature reaction can be evaluated for because of the limited size of the sample being tested and flotation rate of the inclusion. Previous work on the reaction between high aluminum steel and a silica rich slag[42,53,54] has suggested that the kinetics follow a first-order relationship with aluminum diffusion being the rate controlling step through mass transfer in the metal phase [54,42]

The dimple samples allow for different temperature conditions to be investigated to calculate a rate of reaction under different conditions (molten steel and / or inclusion). The dimple tests also gave kinetic data for potentially tracking inclusion composition changes under the different conditions. The dimple tests showed that a reaction does take place when the inclusion is liquid and the steel is semi-solid with the silica content decreasing to 35% of its starting composition after 20 seconds. The reaction was still ongoing but difficult to capture due to the steel becoming fully molten after 20 seconds. It did however allow the inclusion to be investigated when in contact with a liquid steel layer with solid steel.

When casting high aluminium steels, the effect of the mould flux needs to be taken into consideration. The results from this research have shown what the reaction times are and what floatation times are and this could aid in deciding which casting route is appropriate. The ability to employ a correlative study across these different experimental techniques and test methods offers the potential to innovatively understand inclusion behaviour in a highly unpredictable and chemically unstable system.

Table 0.1 Comparison between all the test methods showing the applications, information needed and information that was found and not found as well the success rate of each test method

Test method	Wanted information	What information was found?	What information was not found?	Useful applications of test method	Success rate
Furnace tests	Equilibrium compositions	The crucibles (alumina, zirconia and magnesia) were not useful for this test	No information was found due to the crucibles breaking Compositions dependent on time Equilibrium values	To validate mathematical models to get kinetic and equilibrium compositions of the reaction	Zero due to the crucibles reacting with the mould powder
Powder press	Morphology/compositional information of inclusion/steel reaction when the inclusion is entrained in the steel	Possible to imbed an inclusion	Morphology/compositional information	3D printing	0
Pellet samples	Morphology/compositional information of inclusion/steel reaction when the inclusion is entrained in the steel	Fast heating regime: changes in the morphology of inclusion as a result of compositional changes	Slow heating regime: Morphology/compositional information of the inclusion as the steel did not melt	Useful test method when studying the reaction between the matrix and an entrained particle	15 samples tested, 3 successful to show spontaneous emulsification
Dimple tests	Morphology/compositional information of inclusion/steel reaction at different temperatures that could relate to reactions in the continuous caster	Compositional changes at different temperatures	Morphology of inclusion as a result of compositional changes	Tracking inclusion composition in final slab against continuous casting/process variable locations	All were successful

6. Kinetic Study of Material Exchange

During the manufacturing of steel, many reactions occur at the slag-metal interface [98,99]. This can be of concern for quality control in transformation-induced plasticity steels production due to the reaction between the Al in the molten steel and the silica in the slag [53,54]. Stokes' law for floatation is the principle method for calculating the velocity of a discrete particle rising through a fluid medium. Stokes' law takes into account variables such as viscosity, size and density, however, if a reaction occurs leading to an exchange in material, these variables can change. Therefore, the reaction kinetics between silica rich inclusions and Al containing steel needs to be considered.

6.1 Mathematical model

Mould slag powders contain high levels of silica and presents a challenge when casting high aluminium steels due to the reaction between the dissolved aluminium in the steel melt and the silica in the mould slag. Aluminium is a major alloying element in novel and next generation steels such as TRIP and low-density steels and is added for weight reduction and to aid phase transformation kinetics. However, a decrease in silica in the mould slag causes problems in the continuous casting process as it changes the slag viscosity which is vital for controlling lubrication, with the reaction being shown in Eqn. [3].

The free energy change of a reaction, known as delta G, can show whether or not the reaction will occur spontaneously. Reactions that occur spontaneously have a negative delta G value, and such if a system is at equilibrium, then delta G is zero. One thing to note is that the value of delta G does not provide information on the rate of reaction as delta G of a reaction is the free energy of the final state minus the free energy of the initial state, making it independent of the reaction pathway.

As the reaction at the slag-steel interface is extremely complicated, for this study, the silicon-oxygen and aluminium-oxygen equilibrium (Eqn. [1], [2] and [3]) will be focussed on, simplifying the mathematical model. This model can be applied to other reactions by replacing the appropriate values for the corresponding reactants.

1) $2[Al]_{metal} + 3[O]_{metal} = (Al_2O_3)_{slag}$ [1]
2) $[Si]_{metal} + 2[O]_{metal} = (SiO_2)_{slag}$ [2]
3) $4Al + 3SiO_2 = 2Al_2O_3 + 3Si$ [3]

with the corresponding Gibbs free energy values calculated in Eqn. [4], [5], and [6]:

$$\Delta G_1^\circ = -1205115 + 386.14\,T\ \left(\frac{J}{mol}\right) = -481875\ when\ T = 1873K^{100}$$

[4]

$$\Delta G_2^\circ = -580541 + 220.665\,T\ \left(\frac{J}{mol}\right) = -167254\frac{J}{mol}\ when\ T = 1873K^{100} \quad [5]$$

$$\Delta G_3^\circ = -720680 + 133\,T\ \left(\frac{J}{mol}\right) = -471571\frac{J}{mol}\ when\ T = 1873K^{54} \quad [6]$$

where T is the temperature. The respective equilibrium constants (Eqn. [7], [8], and [9]) are therefore written as:

$$K_1 = exp\left(-\frac{\Delta G_1^\circ}{RT}\right) = \frac{\alpha_{Al_2O_3}}{\alpha_{Al}{}^2 \cdot \alpha_O{}^3} = 2.75\ x\ 10^{13} \quad [7]$$

$$K_2 = exp\left(-\frac{\Delta G_2^\circ}{RT}\right) = \frac{\alpha_{SiO_2}}{\alpha_{Si} \cdot \alpha_O{}^2} = 46195 \quad [8]$$

$$K_3 = exp\left(-\frac{\Delta G_3^\circ}{RT}\right) = \frac{\alpha_{Si}{}^3 \cdot \alpha_{Al_2O_3}{}^2}{\alpha_{SiO_2}{}^3 \cdot \alpha_{Al}{}^4} = 1.42\ x\ 10^{13} \quad [9]$$

where R is the gas constant, $\alpha_{Al_2O_3}$ and α_{SiO_2} are the activities of alumina and silica. The parameters α_{Al}, α_O and α_{Si} are the activities of aluminium, oxygen and silicon dissolved in the steel.

In this system, the mass transports in both the metal and the slag phases are considered. From literature, a mixed control model is preferred as it is valid for all concentrations of aluminium in the steel and for even low concentrations of silica in the slag [42]. From literature, the mixed control model predicts that the rate of reaction is slower due to the added resistance of the metal phase mass transport. When the initial concentration of aluminium in the metal increases, the normalised rate of reaction decreases. The increased aluminium content in the metal slows the reaction due to the limited silica provided to the reaction interface in the mixed control model. The assumptions are that the local equilibrium is achieved at the metal/slag interface and there is no accumulation of the reactant and product at the interface and the material moves away from the interface as shown in Figure 6.1.

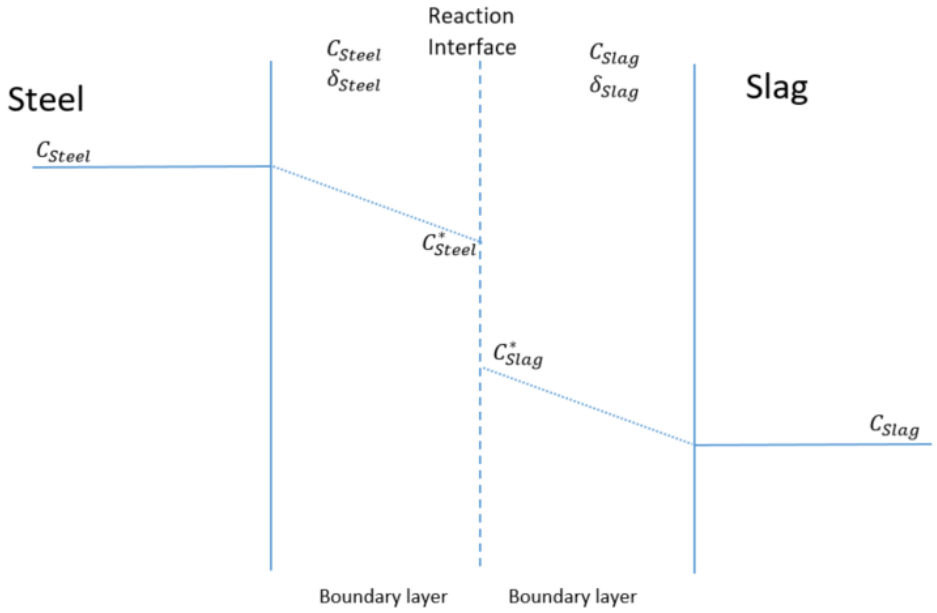

Figure 6.1 schematic composition changes of reaction with time in a mixed control case where this is a compositional gradient of silica

where C_{slag} and C_{steel} is the wt% in the bulk phase of the slag and steel respectively and C^*_{slag} and C^*_{steel} is the wt% at the boundary layer of the slag and steel at equilibrium.

Mass transfer and diffusion equations (Eqn. [10]) are used to calculate the equilibrium compositions of a reacting steel and slag.

$$J_{Steel} = \frac{1}{A}\frac{dn}{dt} = \beta_{Steel}(C_{Steel} - C^*_{Steel}) \quad [10]$$

where A is the interface area (reaction area), β_{Steel} is the mass transfer coefficient in the steel phase which is 3 x 10^{-4} m/s. The mass transfer coefficients for steel and slag were taken from literature [42].

From here, the total reaction rate constant is used to calculate the resistance of the reaction which can then be used to determine what exactly the controlling step of the reaction is. It is determined that mass transfer and diffusion is the controlling step rather than a chemical reaction. Using this, the concentration is converted to mass fraction to be able to calculate that the metal diffusion is the controlling step. All of this put together and using stoichiometry and mass balance, gives the graph in Figure 6.2 showing that the reaction reaches equilibrium at 50 seconds.

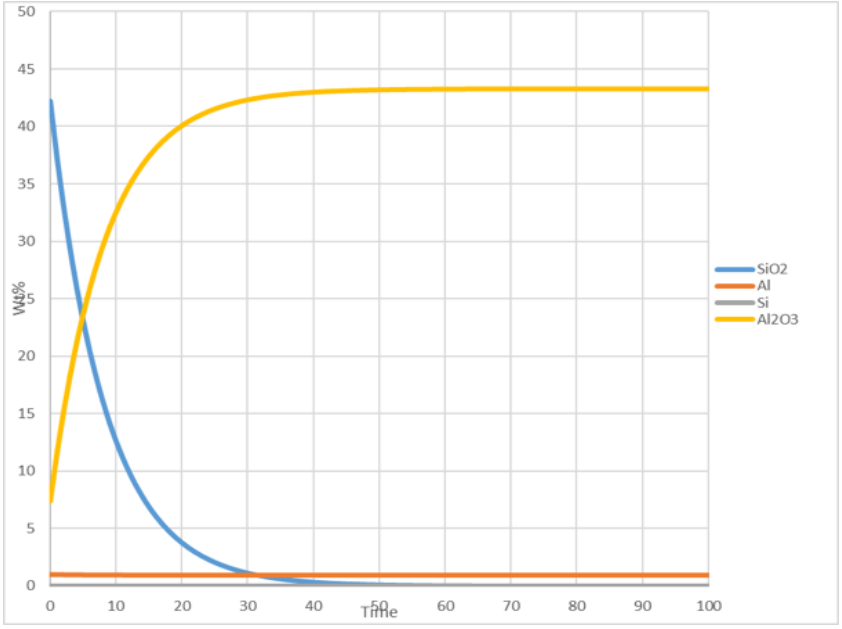

Figure 6.2 Mathematical model output showing the time it takes a reacting inclusion to reach equilibrium

Figure 6.2 shows that an inclusion particle of 450 microns would reach equilibrium in less than 60 seconds assuming that the particle stays the same shape and size, and only the composition and therefore density and viscosity changes.

6.2 FactSage

Further validations were completed using FactSage which verified that the silica content in the slag reaches near zero as shown in Figure 6.3. The advantage of the mathematical model is that it gives kinetic data and a time value for the reaction reached whereas FactSage only gives composition data.

```
(1600 C, 1 bar,     a=1.0000)
( 56.571     wt.% Al2O3
+ 6.8233E-02 wt.% SiO2
+ 43.285     wt.% CaO
+ 2.8666E-03 wt.% FeO
+ 1.2151E-05 wt.% Fe2O3
+ 2.8503E-04 wt.% MnO
+ 3.0399E-02 wt.% B2O3
+ 5.0764E-03 wt.% Ti2O3
+ 1.2009E-02 wt.% TiO2
+ 5.3059E-08 wt.% Mn2O3
+ 1.4837E-02 wt.% Al2S3
+ 1.8649E-05 wt.% SiS2
+ 9.9169E-03 wt.% CaS
+ 6.2465E-07 wt.% FeS
+ 2.8169E-09 wt.% Fe2S3
+ 6.2256E-08 wt.% MnS
+ 9.1614E-06 wt.% B2S3
+ 1.2072E-06 wt.% Ti2S3
+ 2.9991E-06 wt.% TiS2
+ 1.2334E-11 wt.% Mn2S3)
```

Figure 6.3 FactSage outputs for the reaction showing that silica reaches a similar amount as the mathematical model

The experimental data from these tests show that the reaction has not yet reached completion. Due to the nature of the tests and the inclusions having a tendency to float (pellet samples) or the interface between the inclusion and steel being difficult to monitor if the steel has completely melted (1873 K dimple samples), this point is difficult to reach.

6.3 Dimple samples

The purpose of this study is to identify the kinetics for the chemical reaction and the time for the silicon and aluminium contents in the inclusion and steel to equilibrate under different conditions, namely liquid inclusion – liquid steel, liquid inclusion – solid steel and solid inclusion-solid steel. The rate of reaction for the liquid inclusion – liquid steel condition will have an effect on inclusion residence time in the liquid steel due to chemical drag, and composition/density changes.

The silica and alumina contents in the inclusion as a function of time from the quenched-sectioned samples are presented in Table 3. The table shows that the silica content decreases as the alumina content increases in the inclusion as the reaction (equation 1) progresses. Previous work on the reaction between high aluminium steel and a silica rich slag [14,17] has suggested that the kinetics follow a first-order relationship with aluminium diffusion being the rate controlling step through mass transfer in the metal phase [54,42].

6.3.1 Results

Heat treatments in the HT-CLSM, under a gas environment that was inert with respect to the system, were used to enable a controlled reaction time between the liquid metal and slag phases under near isothermal conditions.

6.3.1.1 1473 K – solid steel, liquid inclusion

Figure 6.4 shows the SEM images of the heat treated samples at 1473 K at 30, 900 and 1800 seconds. This test allowed for the inclusion to be liquid and the steel to remain solid to examine the liquid-solid reaction. These images show the position of the inclusion in the indent in the steel matrix.

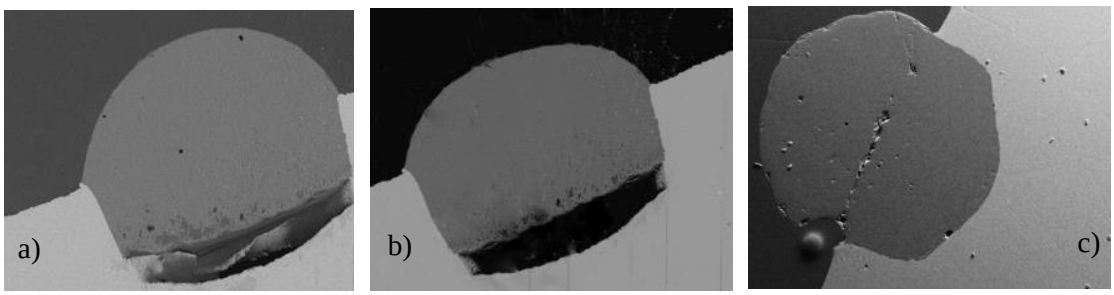

Figure 6.4 SEM image of the heat treated sample at 1473 K a) 60 seconds b) 900 seconds c) 1800 seconds

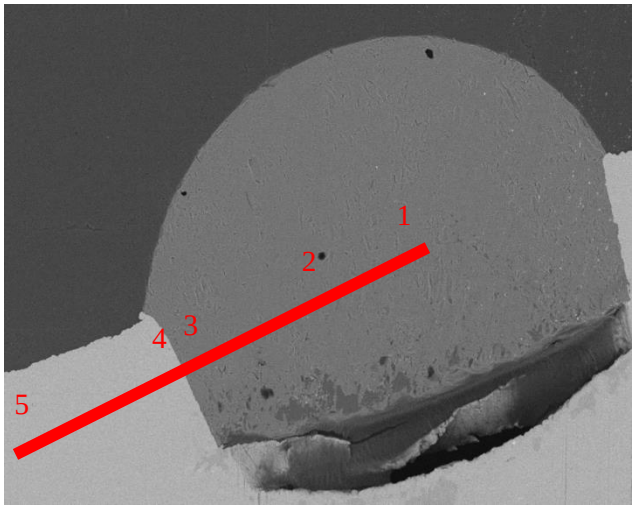

Figure 6.5 SEM image of the 60 second sample at 1473 K

Table 6.1 The point analysis showing the composition of Al and Si in wt%

	Al	**Si**
1	7.5	42.0
2	7.5	42.0
3	7.6	41.9
4	1.0	0.0
5	1.0	0.0

Figure 6.4 and 6.5 shows the 60 second sample and 90 second sample with the point composition analysis of the inclusion and the steel. It shows that, for the condition examined where the inclusion is liquid during the test, it has a homogeneous composition. The steel composition does not change noting that the steel is still solid and in excess compared to the volume of the inclusion. There is a decrease in silicon and increase in aluminium in the inclusion at 900 seconds suggesting that the liquid inclusion could be reacting with the steel at the interface as shown in Figure 6.6 and Table 6.2.

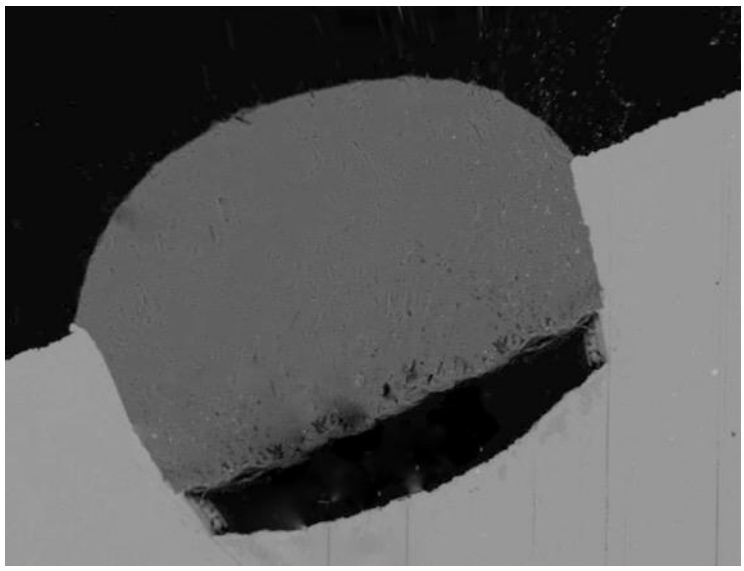

Figure 6.6 SEM image of the 900 second sample at 1473 K

Table 6.2 The point analysis showing the composition of Al and Si in wt%

	Al	**Si**
1	1.0	0.0
2	11.2	38.4
3	11.3	38.3
4	1.0	0.0
5	1.0	0.0

6.3.1.2 1873 K – semi-solid steel, liquid inclusion

Figure 6.7 shows the SEM images of the heat treated samples at 1873 K at 5, 10, 15 and 20 seconds. This test allowed for the inclusion and the steel to be liquid. For tests with hold times greater than 20 seconds the steel melted completely giving mixing with the inclusion leading to the loss of a distinguishable interface to observe.

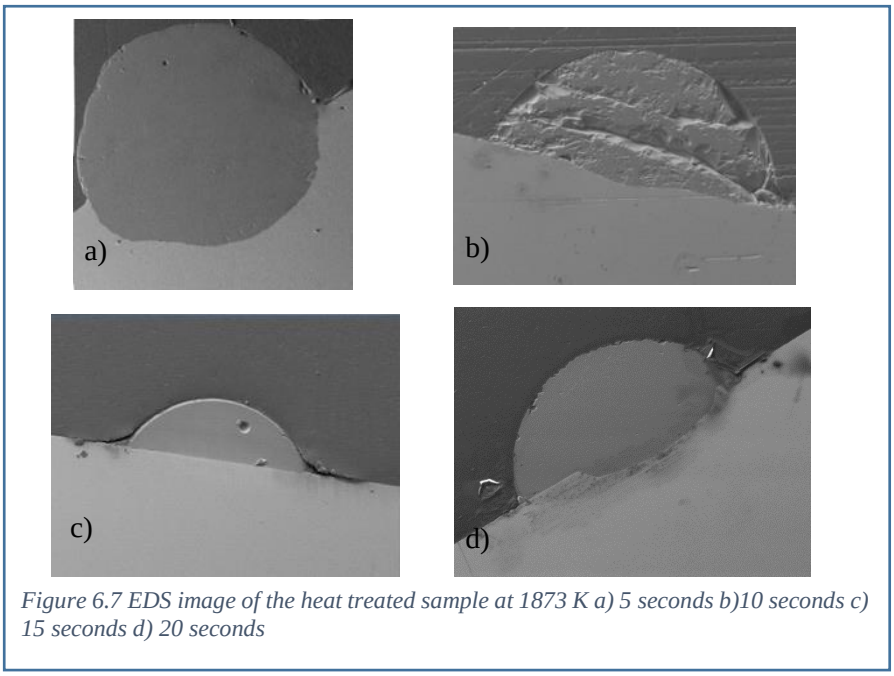

Figure 6.7 EDS image of the heat treated sample at 1873 K a) 5 seconds b)10 seconds c) 15 seconds d) 20 seconds

Figures 6.8 and 6.9 show the SEM image of the 5 seconds and 20 second samples respectively at 1873 K with the corresponding point analysis showing the compositions of aluminium and silicon shown in Table 6.3 and Table 6.4. The inclusions in both samples are homogenous as there is no compositional gradient, and the concentration of Si decreases over time with the Al concentration increasing. The steel composition does not change which could suggest that the reaction is happening at the interface between the steel and the inclusion with rapid diffusion in the inclusion and steel. The aluminium in the steel is also in excess so the change would be extremely small. Table 6.5 shows all the compositions of the different samples over time.

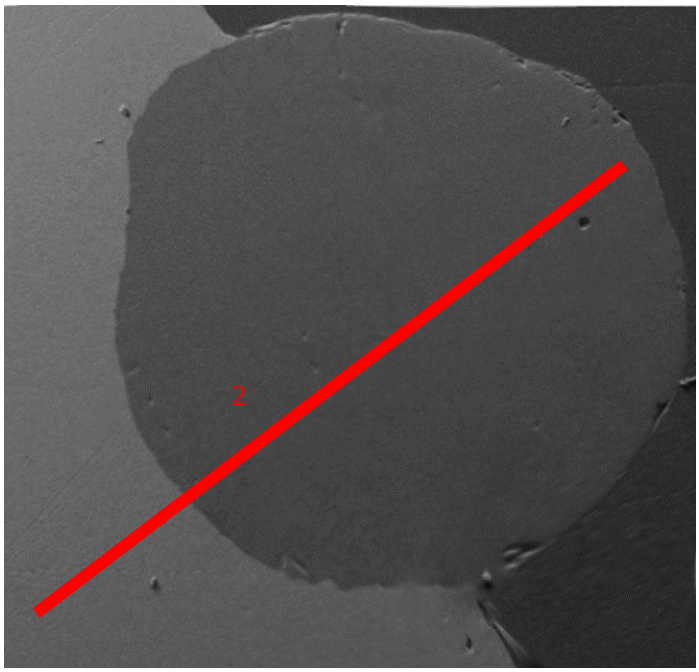

Figure 6.8 SEM image of the 5 second sample at 1873 K

Table 6.3 The point analysis showing the composition of Al and Si in wt%

	Al	Si
1	24.3	25.2
2	24.4	25.1
3	1.0	0.0
4	1.0	0.0
5	1.0	0.0

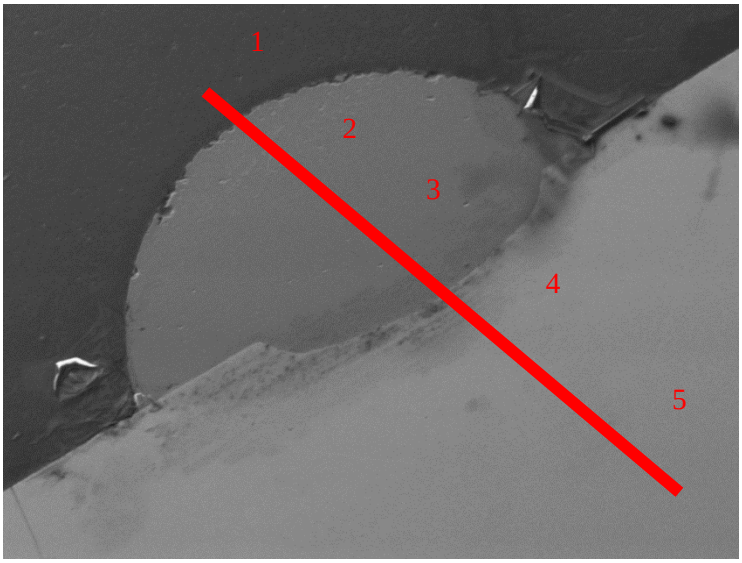

Figure 6.9 SEM image of the 20 second sample at 1873 K

Table 6.4 The point analysis showing the composition of Al and Si in wt%

	Al	Si
1	34.6	14.9
2	34.7	14.8
3	34.6	14.9
4	1.0	0.0
5	1.0	0.0

Table 6.5 The silica and alumina content in the inclusion with respect to time (all wt %)

Time (s)	1473 K		1873 K	
	Si (wt%)	Al (wt%)	Si (wt%)	Al (wt%)
0	42.1	7.4	42.1	7.4
5	42.1	7.4	25.2	24.3
10	42.0	7.5	20.8	28.7
15	42.1	7.4	18.2	31.3
20	42.0	7.5	14.9	34.6
60	42.0	7.5	-	-
90	41.8	7.7	-	-
120	41.2	8.3	-	-
180	40.8	8.7	-	-
240	39.8	9.7	-	-
360	39.4	10.1	-	-
420	38.7	10.89	-	-
900	38.4	11.2	-	-
1800	37.8	11.8	-	-

Studying the reaction of the inclusion and the steel at different temperatures could allow us to calculate a rate of reaction at different points in the continuous caster. Figure 6.10 shows where the steel is solid, mushy and liquid, will all have different reaction rates and compositions when reacting with a silica rich inclusion from the slag layer. If an inclusion is detected in the final product, based on the composition, the reaction time of the inclusion could be estimated.

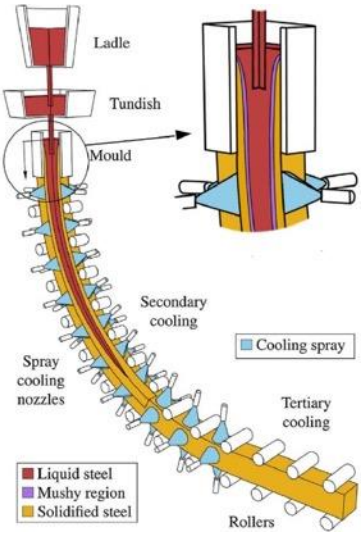

Figure 6.10 Schematic diagram to show the steel in the continuous caster where the steel is in three states : solid, liquid and mushy [6]

7. Spontaneous emulsification of entrained inclusions during Casting of High Aluminium Steels

7.1 Introduction

As discussed in previous chapters and submissions, mould slag particles that remain in the liquid steel after the continuous casting process have a high likelihood of ending up in the final steel slab. Inclusion morphology and compositions are affected by the reaction between the inclusion and the steel. Inclusions need to be controlled in terms of their size, number distribution and morphology such that the probability of removal by flotation is high and also they do not result in critical product defects or cause problems with process flow [7].

In this chapter, the interaction between mould slag inclusions and liquid steel of two compositions (low, 0.04 wt%, and high, 1 wt%, Al content) is considered to determine reaction kinetics and any changes to the inclusion particle size and morphology. Further information can be found in Submission 5: The Spontaneous Emulsification of Entrained Inclusions during Casting of High Aluminum Steels [97]. The use of the HT-CLSM and XCT have been used successfully before to investigate metal droplets in slag [84,85,101,102]. The same techniques will be applied for this study combining it further with SEM/EDS techniques to allow an inclusion that was fully immersed in the liquid steel to be located in a quenched sample and non-destructively characterised for morphology before subsequent destructive characterisation. The non-destructive characterisation is unique and a significant step to studying the morphology of a reacting inclusion within the steel matrix, allowing for important information about the reaction interface to be investigated. Historically, previous studies have relied on dissolving the steel matrix or examining layers of mould slag on the liquid steel [103].

7.2 Results

7.2.1 1 wt. % aluminium

Figure 7.1 shows the XCT images of the samples before and after heat treatment at 1893K of 5, 10, and 20 seconds for the 1 wt% Al steel. The results shown can be interpreted as the evolution of the inclusion as a function of time from 0 (a starting condition) to 20 seconds. The inclusion appears to break apart into smaller particles at5 seconds as seen in Figure 7.1b and then start to recombine to one large particle with very few smaller particles in Figure 7.1d.

The XCT scan (Figure 7.1b) of the 5 second hold sample indicated that the inclusion had broken up into many small particles (i.e. emulsified) but the resolution of the scan was not sufficient to see this in detail, therefore the sample was sectioned in the area of interest and observed under SEM. The SEM image, as shown in Figure 7.2a, shows the many small inclusion particles. EDS analysis showed that these are inclusions with silica contents of an average of 17.9±1.5%. EDS analysis of the steel in the area between the emulsified small inclusion particles shows that the aluminium content has reduced to 0.36 wt. %, compared to the global aluminium content being still near to 1 wt. %.

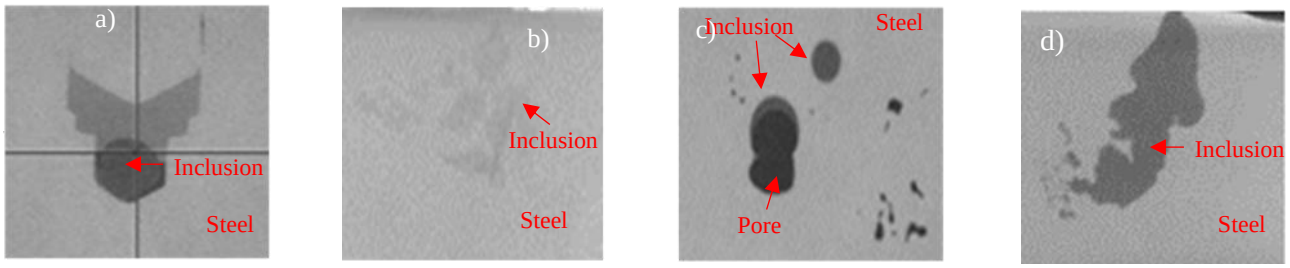

a) Pre-heat treatment b) 5 sec c) 10 sec d) 20 sec

Figure 7.1 (a) - (d) XCT slices showing the evolution of the inclusion immersed in steel as a function of time in 1 wt. % Al steels

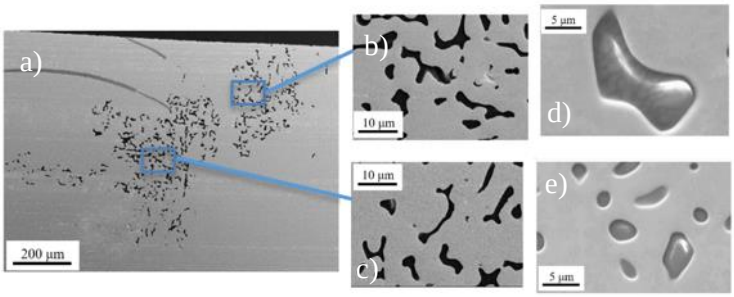

Figure 7.2 a) 5 seconds hold emulsified sample under SEM with b) and c) at a higher resolution showing a clearer image of the shape of the inclusions, d) an inclusion of approximately 10 micron size, e) inclusions of approximately 5 micron size

Figure 7.3 shows a 3D XCT reconstruction of the ten seconds hold sample and SEM and EDS maps of the large inclusion obtained after sectioning the sample in the area of interest identified from the XCT scan. The EDS maps show the presence of silicon, aluminium and calcium in the oxide mixture. Further point analysis showed the silica content had reduced to 9.8 wt. % and the alumina concentration had increased to 42.52 wt. %. Using FactSage to compute the change in crystallization temperature of the inclusion as a result of this compositional change shows that the melting/solidification temperature increases from 1531 K (starting composition) to 1605 K.

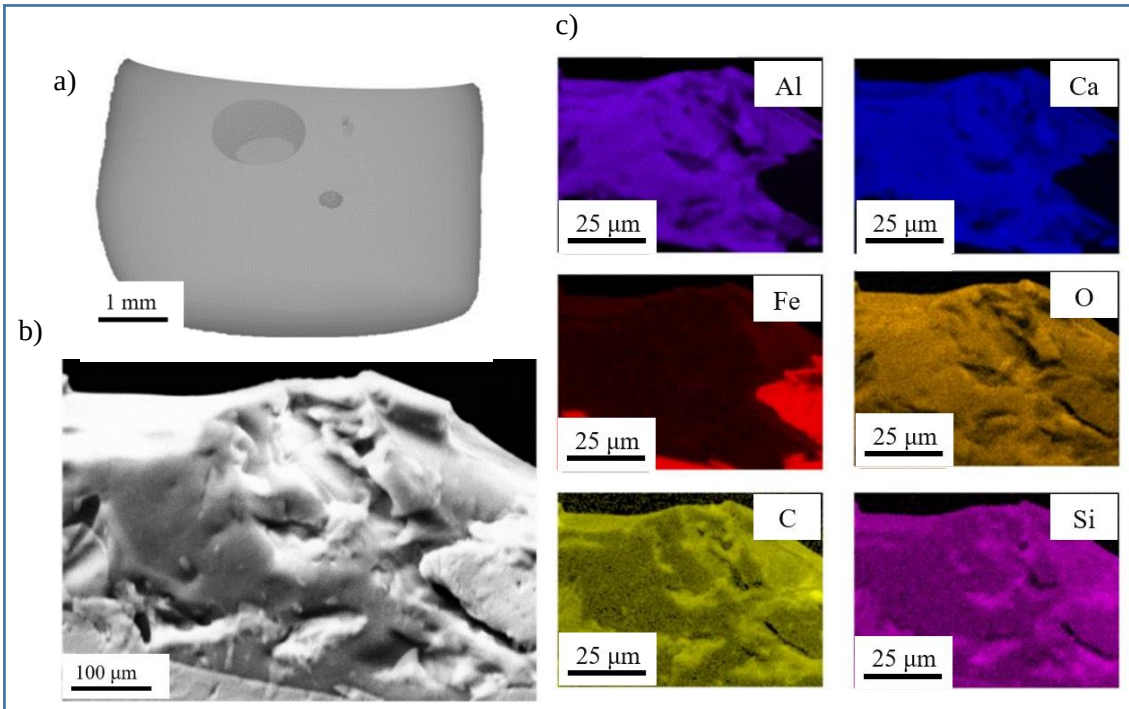

Figure 7.3. The 10 second hold 1% sample a) 3D reconstruction of the sample from XCT data, b) SEM image of the inclusion area, c) map scans showing elemental composition of the area in view

Figure 7.4a shows the 3D XCT reconstructed coalesced inclusion within the steel matrix at 20 seconds. Figure 7.4b is an SEM image of the inclusion. The silica content in this inclusion was found to have reduced to 2.8 wt. % and the alumina content increased to 46.84 wt. %. The inclusion is one particle at the top centre of the sample, although the SEM image shows multiple particles due to a sectioning effect.

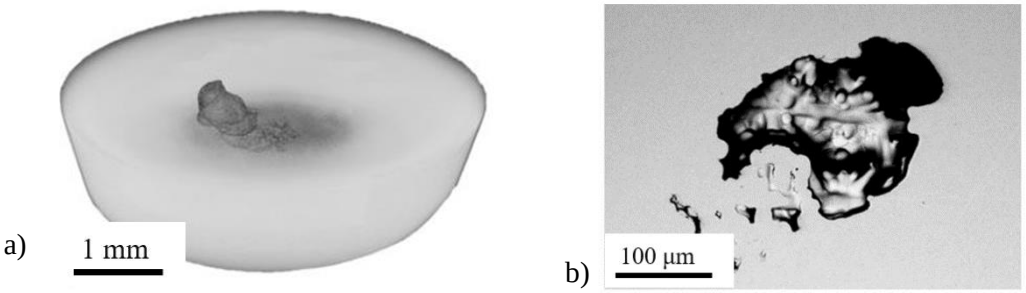

Figure 7.4 20 second hold sample a) 3D reconstruction of the sample showing the coalesced inclusion within the steel matrix, and b) SEM image of the inclusion taken from the sectioned sample through the area of interest.

The silica and alumina contents in the inclusion as a function of time from the quenched-sectioned samples are presented in Table 7.1.

Table 7.1 The silica and alumina content in the inclusion with respect to time (all wt %)

Time (s)	**SiO_2**	**Al_2O_3**
Pre-melting	42.1	7.4
5	17.9	31.7
10	9.8	42.5
20	2.8	46.8

The interfacial area between the metal and slag phases of samples treated for various times has been calculated using Avizo, a 3D visualization software, and is presented in Table 7.2.

Table 7.2 showing the change in surface area of the inclusion(s) with respect to time, with A0 being the initial surface area and Ai being the surface area at any given time point.

Time (s)	**Surface area (mm^2)**	**A_i/A_0**
Pre-melting	0.6361	1.000
5	8.445	13.27
10	0.7854	1.234
20	0.6648	1.045

7.2.2 0.04 wt. % Aluminium

A low aluminium steel (0.04 wt. %) was also investigated using the same test methods. The inclusion is seen to remain as one particle and not emulsify for each of the time steps investigated. This is shown in the XCT images in Figure 7.5. The corresponding silica and alumina wt % of the inclusion as measured via SEM-EDS is given in Table 7.3. The composition is seen to stay relatively constant consistent with there being little reaction potential between the two phases in this system.

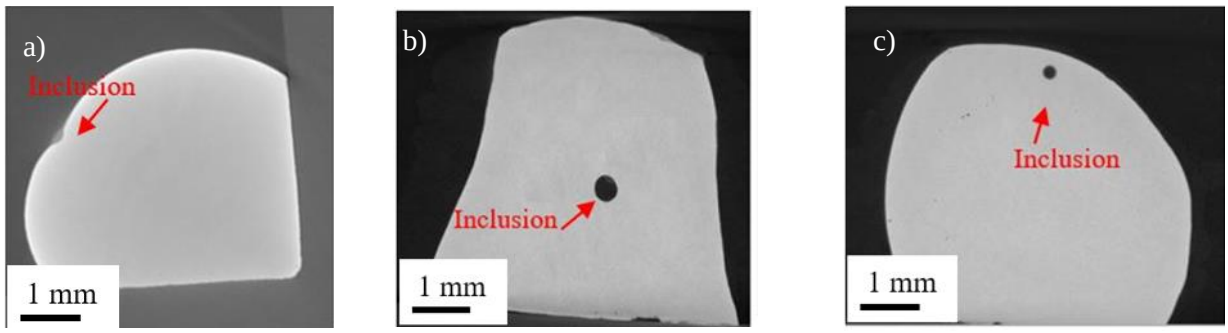

Figure 7.5 0.04 wt. % aluminium steels showing the inclusion to be one particle throughout the test a) 5 seconds b) 60 seconds c) 300 seconds

Table 7.3 showing the composition of the inclusion in the 0.04 wt. % samples at five seconds, 60 seconds and 300 seconds.

Time (s)	SiO_2	Al_2O_3
5	42.1	7.4
60	41.8	7.2
300	42.0	7.3

7.3 How Spontaneous Emulsification occurs

The reaction in Eq. [1] has a negative Gibbs free energy for both of the starting systems (high and low Al steels), so the forward reaction is favourable and there is a driving force for the reaction to proceed. Dynamic interfacial phenomena, i.e. spontaneous emulsification, was observed for the 1 wt. % Al steel sample but not in the low-Al steel sample. A schematic of the progression of spontaneous emulsification, for the high Al-steel sample is shown in Figure 7.6, following the understanding presented previously in the literature for a high temperature mass transfer driven phenomenon occurrence [104].

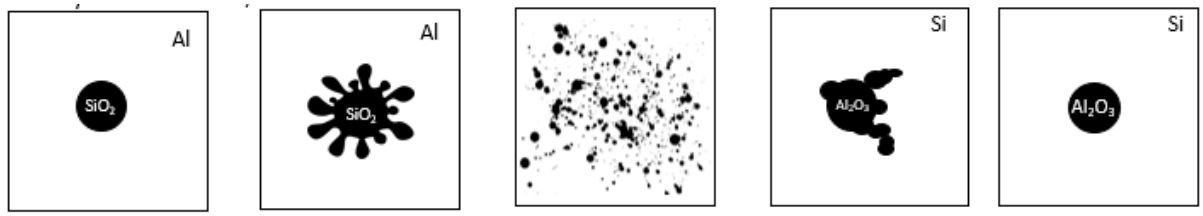

Figure 7.6 Schematic of spontaneous emulsification with initial conditions of silica in the inclusion and aluminium in the steel.

The results suggested spontaneous emulsification has occurred in these samples, which is driven by the chemical reaction between the aluminum in the steel and the silica in the slag particle. In the 0.04% Al samples, it is seen that the inclusion stays as one particle with little to no change in the inclusion chemistry. To form an emulsion, and to sustain an emulsion (increase in interfacial area), there needs to be an increase in material exchange between the steel and the inclusion. As the chemical potential in the low Al system is much lower, it is not enough to form an emulsion. This is why this behaviour is seen in the 1%Al system as there is enough of a chemical potential. This has been seen before in the literature, but under different circumstances where it was a metal particle in a slag, involving a reaction where phosphorus was present [101]. This is the first time spontaneous emulsion has been seen with a slag particle in bulk metal, but it does follow a similar pattern of requiring the chemical reaction to sustain the increase in interfacial energy as a result of the emulsification process.

7.4 Effect of Spontaneous Emulsification on inclusion behaviours

Spontaneous emulsification will affect inclusion flotation velocity as smaller inclusions will float slower than larger inclusions. Inclusions with a starting size of 450 micron size that is silica rich, would have a floatation velocity of 0.167 m/s (according to Stokes' law). As the reaction progresses and emulsifies, a particle of 10 micron size (considering similar composition, and hence density) would float at $7.33 \cdot 10^{-5}$ m/s, reducing the floatation velocity significantly to a point where it is almost

negligible. As the inclusion particle coalesces, and the inclusion becomes alumina rich, the velocity of the reported inclusion would be 0.149 m/s. Assuming Stokes' floatation in a continuous caster where a mould flux inclusion is entrapped at the top of the continuous cast mould, giving a flotation distance of 30 meters for inclusion removal to the slag layer then an inclusion that is silica rich of 450 micron initial size would take 180 seconds to float out, however, an inclusion that has reacted that is now alumina rich of the same size would take 201 seconds to float out, which is an increase of 11.7%. Taking the reaction into account giving a short time frame where an emulsion exists, an inclusion that undergoes these dynamic changes would take 203 seconds to float, which is an increase of 12.7%. However, coalescence rates in the continuous caster are expected to be less than that seen in the HT-CLSM experiment (due to fluid flow and turbulence) and these effects could greatly increase the flotation time. Spontaneous emulsification would undoubtedly affect inclusion floatation in the continuous caster as smaller inclusions have less buoyancy than larger inclusions.

Figure 7.7 shows the changes in silica and alumina content in the inclusion with relation to the changes in the ratio of the surface area. As the reaction progresses, there is a decrease in the driving force of the reaction as the chemical potential reduces leading to a reduction in the reaction rate.

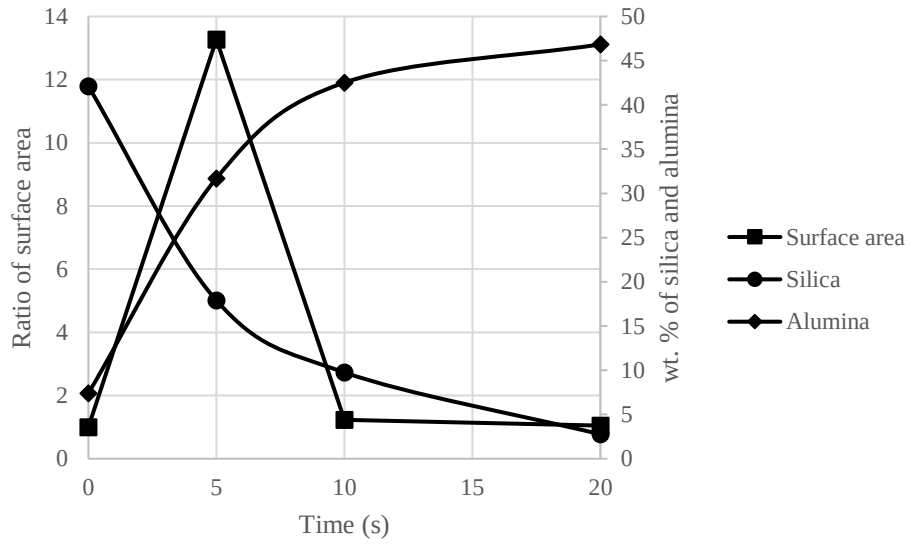

Figure 7.7 The change of alumina and silica content in the inclusion during the reaction with the change in surface area

8. Reflections to Industrial Practice

8.1 Why is inclusion behaviour important?

Thermodynamics has also played a huge part in the development of inclusion engineering and clean steel [105,106]. The characteristics of inclusions are also important, whether they are hard or soft, also have an effect on product fatigue, strength and corrosion [107]. Density and viscosity can affect floatation behaviour[54]. Available modelling tools have improved significantly with the use of computational fluid dynamics, meaning inclusion control in steels can be developed on a scientific basis to improve process development. Key aspects (morphology changes such as spontaneous emulsification and kinetics of slag-metal reactions) linked to the fundamental behaviour of inclusions are unknown and as such CDF models require validation from laboratory investigation as to how to treat inclusions during situations such as teaming, turbulent and counter flow velocity situations [72,108].

The changes in morphology of the reacting inclusion could affect inclusion floatation in the continuous caster. In a thin slab caster, the liquid steel takes approximately two minutes to solidify and in a thick slab caster it takes approximately seventeen minutes to solidify [3]. These times are much longer than the reaction times for the inclusion and the steel that have been reported in Chapters 6 and 7 (20 seconds) but not longer than the reaction time that has been calculated (50 seconds), showing that reactions could happen quicker than expected. As a steel slab solidifies from the mould contact surface towards the centre of the slab, an inclusion that is found on the steel surface would have had less time for reaction with the liquid steel, whereas an inclusion in the middle of the steel slab could have had more time for reaction, and for floatation.

8.2 Inclusion defects in products - Battery cans

Tata Steel Europe, Ijmuiden, produce nickel-coated steel strip that is specifically developed for battery applications. It is created by electroplating cold-rolled battery quality ultra-clean steel grade with nickel and diffusion annealing. However, some defects have been found on the surface of these battery cans and it is believed they are caused by inclusions arising during steelmaking. The battery cans shown in Figure 8.1 were produced by a deep drawing process (shown in Figure 8.2) where a sheet of steel is stretched over a form or a die. The nickel-plated sheet of steel is cut into a circle of an adequate size for making the desired part. The blank holder holds the sheet metal in such way that it can form into the die. The blank is drawn into the die by a rigid punch, which forces the sheet to take the shape of the punch. This is shown in Figure 8.2 below, showing the deep drawing process and the different parts.

Battery can samples were inspected visually as shown in Figure 8.1, as well as using electron microscopy. The SEM used for microscopic investigations was a Zeiss Supra 55VP and EDX was carried out to identify the chemical compositions of any inclusions present in the parabolic lines. 13 battery can samples were analysed, 8 of which showed the presence of some inclusion particles within the parabolic lines. It is theorised that for those where no inclusions were detected, that during treatment and transit poorly bonded inclusions would have a high chance of being dislodged from the sample.

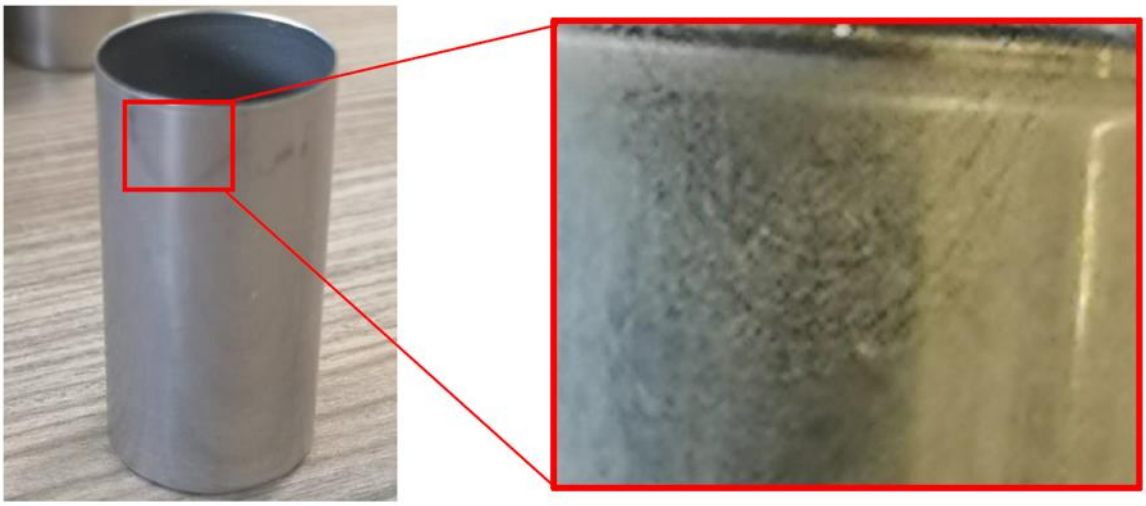

Figure 8.1 Battery cans showing the parabolic line defects caused by inclusion

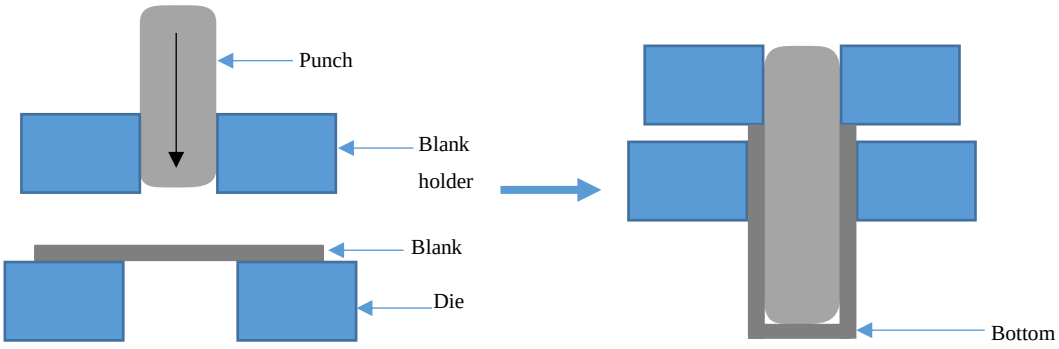

Figure 8.2 Schematic drawing of the deep drawing process and the different parts required the black arrow indication the direction of the punch.

Figure 8.3 shows a section of the parabolic lines under SEM and the red box indicating the area in which Figure 8.4 shows where the steel is showing through the nickel coating with oxygen and carbon contamination. Figure 8.4 shows the presence of inclusion within the parabolic lines with the EDX map scans. It also shows evidence of calcium, silicon, aluminium and oxygen, expected to be in the form of calcia, silica and alumina with compositions 2.07 wt. %, 32.82 wt. % and 11.14 wt. % respectively.

This composition mix is not indicative of mould powders causing these inclusions as shown in Table 4.2. Na and Cl composition maps are shown to check for any other possible contaminations.

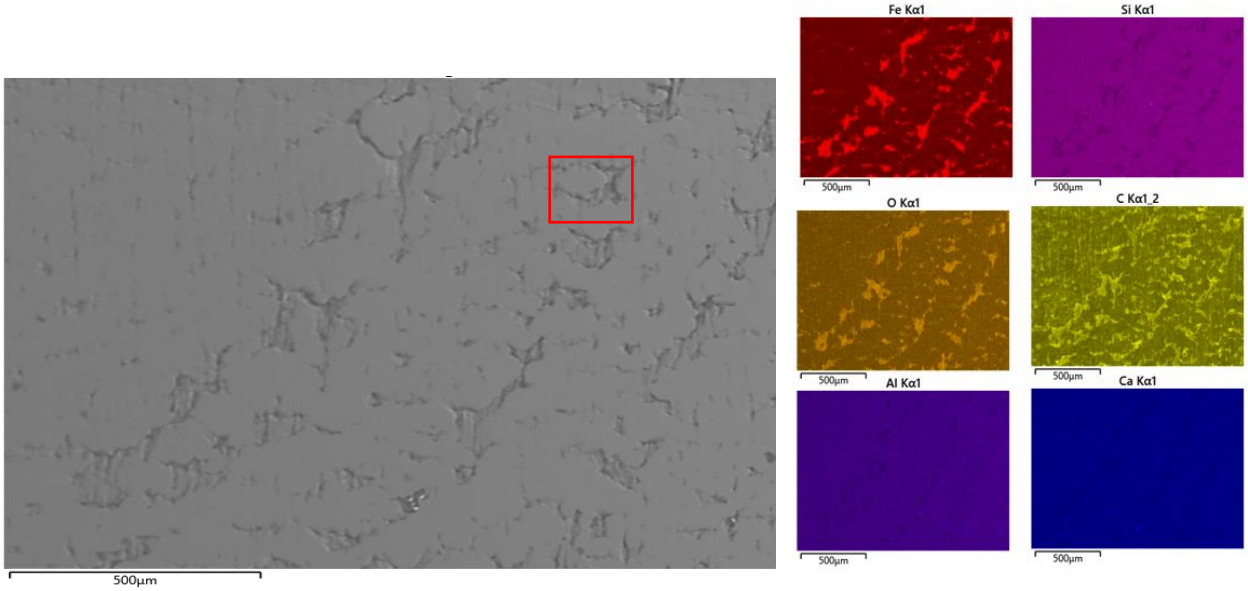

Figure 8.3 Parabolic line under SEM with the red box indicating where the higher resolution inspection was down as shown in Figure 8.4.

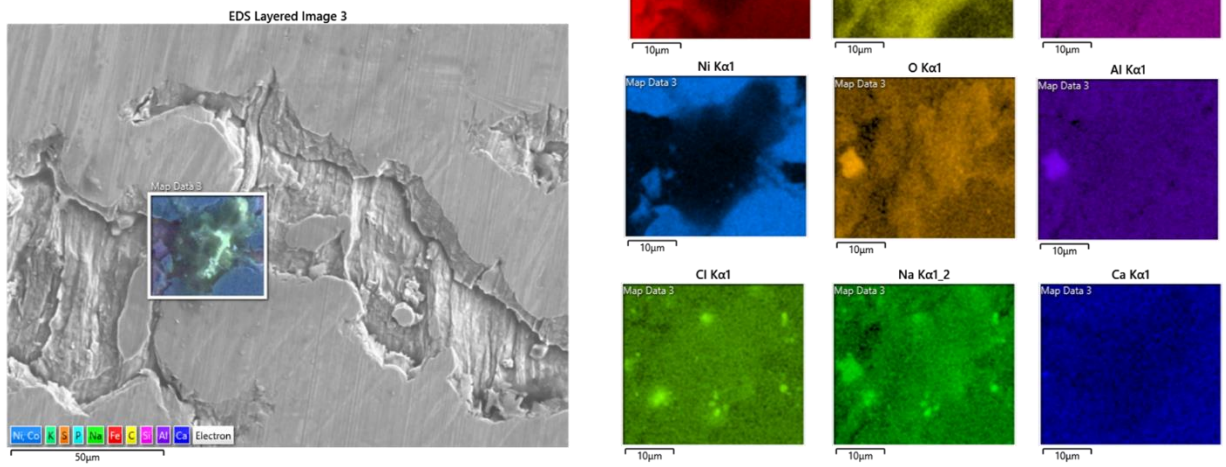

Figure 8.4 A section of the parabolic line where there are some silicon and aluminium present as shown in the EDS map scans

8.2.1 Potential pathways for parabolic defect lines to occur

Non-metallic inclusions can have an adverse effect on rolling and further processing such as deep drawing and coating of the finished steel product causing defects such as line defects and slag spots. Inclusions can give rise to stress concentrations, so when the steel is deep drawn, it can cause cracks.

As the steel is nickel plated, any areas of defects or inclusions are not nickel-plated. This could explain the parabolic lines that have been observed in the direction of deep drawing. There are two possible pathways shown in Figures 8.5 and 8.6 for the parabolic lines to form on the battery cans – line defects or inclusions / slag spots on the cold rolled sheet steel, according to the literature [4]. Line defects are believed to be caused by non-metallic inclusions caught near the surface of the slab, less than 15 mm from the surface [5]. As the nickel will not adhere to these defects, it causes these elongated lines when deep drawn, forming these parabolic lines in the direction of the deep drawing process.

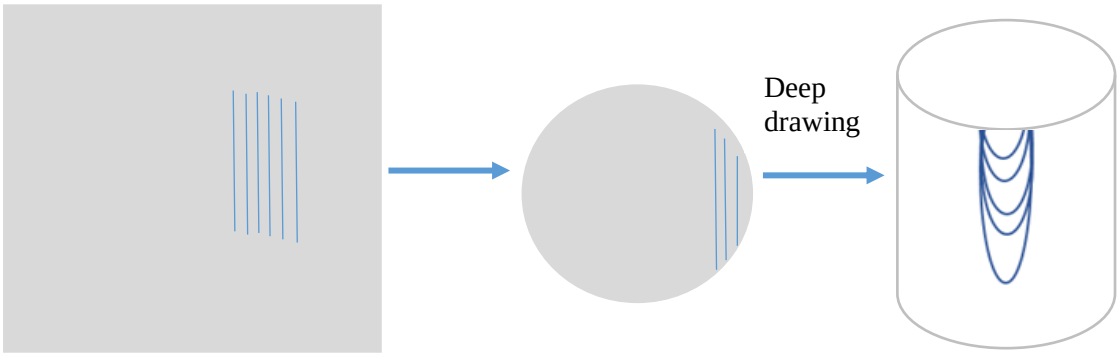

Figure 8.5 Line defects on cold rolled sheet steel causing parabolic lines on battery cans

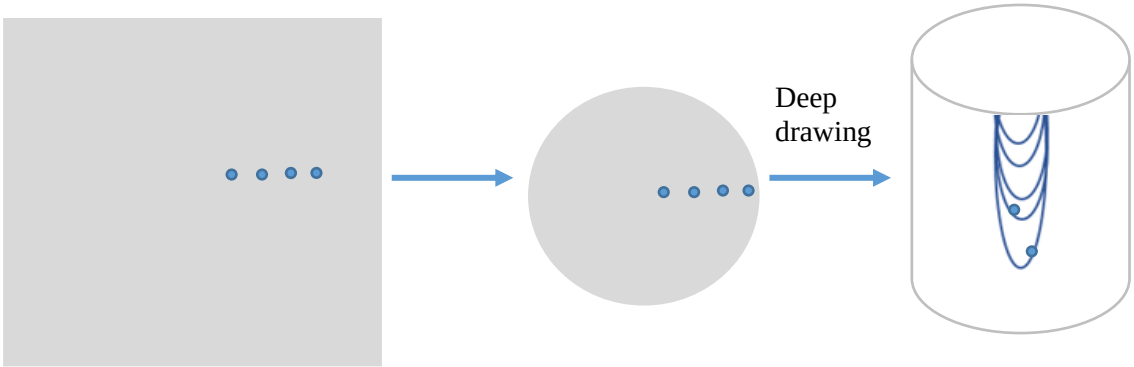

Figure 8.6 Inclusion or slag spots causing parabolic line on battery cans

The inclusions found on the battery cans were found in the parabolic lines and not anywhere else on the surface of the cans, and not all at the bottom of the parabola as expected. This could be from the inclusions initially not being in a straight line as shown in Figure 8.7 and being in more of a dispersed orientation.

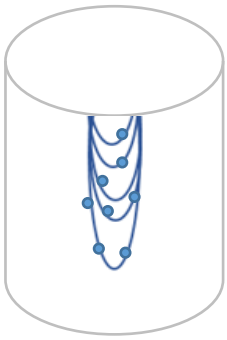

Figure 8.7 The placement of the inclusions that were found within the parabolic lines across the samples

Inclusions can occur at or near the surface of the slab if they become entrapped in the solidifying steel early. During rolling, inclusions can be deformed such as SiO_2 and MnS, which can end up elongated [109], or break up to form stringers. Inclusions can deform when rolled from as-cast slab. This could suggest that the inclusion could have been a soft inclusion cluster that has been strung out during rolling or a hard crystalline inclusion broken during rolling. Alumina inclusions do not deform under rolling, whereas the steel around the inclusion will continue to deform. The direction of the parabolic lines could be an indication on the material flow during the forming step as shown in Figure 8.5.

The average compositions of the inclusions found within the parabolic lines contains 15.2 wt. % alumina, 33.4 wt. % silica, 0.06 wt. % calcia which are different to the mould powder that is used. Therefore it can be concluded that mould powder inclusions are not the cause of the inclusions and defects in the battery cans. As the steel is also a low aluminium steel, there should be little to no reaction between the aluminium in the metal and silica in the mould powder.

The composition of the ladle slag has an average of 8.9 wt. % silica and 34.9 wt. % alumina and 23.7 wt. % of calcia, further showing that these inclusions are not from ladle slag either so this can also be ruled out as a potential for the source of these inclusions in the deep drawn steel.

8.3 How can this knowledge on slag-metal reactions be used?

8.3.1 Mould Flux Design

Due to the reaction between aluminium in the liquid steel and silica in the mould flux that results in changes in composition, properties and performance of the flux as well as potentially causing inclusions that are not removed by flotation which affects slab quality, there has been an increased study of appropriate mould fluxes for continuous casting of high-aluminium steels [110]. As previously discussed, the reaction causes an increase of alumina and a decrease of silica in the mould flux with an increase of

silicon in the steel as well as the morphology changes this can induce in the form of spontaneous emulsification. There is an incentive to develop a less-reactive mould flux that still has the same properties of low viscosity and melting point, and crystallisation properties that will still continue to be appropriate for heat transfer and lubrication to produce a high quality slab with good surface quality [110].

Several researchers have developed mould slags for high aluminium steels (1.5 to 2.5 wt pct of Al) where silica was partially replaced with alumina [110]. Other compositions with different ratios of calcia and alumina for high aluminium TRIP steels [111] or fluoride-free and low-fluoride lime-alumina-based fluxes [112] have also been investigated. These slags were evaluated based on their viscosity, crystallization and effects on steel quality. Yan *et al*. [110], concluded that a calcia/alumina mould slag with a ratio between 1.1 and 1.6 was ideal as it had a low viscosity, low crystallization temperature, and good heat transfer properties which is appropriate for casting high-aluminium steels.

This research has allowed focus for parallel research on new fluxes for high aluminium steels. Tata Steel Europe currently produce 0.7 wt. % aluminium steels so the effect of the mould flux needs to be taken into account when producing even higher aluminium steels. This study has shown the implications of using a silica rich slag and its reactions with high aluminium steels. TWIP and TRIP steels are high aluminium steels, often exceeding 1 wt. % aluminium, and are potential future product Tata Steel wish to bring to their portfolio. The mould powder that was used in this study is not suitable because of the rate of reaction and formation of an emulsion, which could result in lots of inclusions being retained in the steel slab. The results from this research have shown what the reaction times are and what floatation times are and this could aid in deciding which casting route is appropriate (thin slab casting or thick slab casting). This provides information that is relevant for the steel grades that Tata Steel Europe produce for current steels as well as future steel design.

8.3.2 Inclusion Analysis in steel defects

The results in this study can be used to analyse the defects in steel and inclusion compositions can be used to calculate how long the inclusion had reacted for and how long it had remained liquid. Inclusions on the surface or near the surface have a much lower reaction time in the liquid steel than an inclusion in the middle. If micro inclusions are found in the slab or the final product, spontaneous emulsification could be an indication if clouds of reacted micro inclusions are found dispersed throughout the steel and due to turbulent conditions, could not coalesce. This could cause a problem in sheet steel products such as battery cans or automotive products.

This understanding of where and what inclusions might be is helpful for adapting process parameters and conditions. Inclusions could be used as markers; however, a sufficient amount needs to be found to track this. If found, it allows effects such as casting speed, tapping temperature and environmental

condition to be correlated against the observation of these inclusions in the product, and the feedback loop of effect of control can be monitored to a more accurate extent.

8.3.3 Modelling

This research provides information that could be used in CFD models for fluid flow in the continuous caster to understand inclusion behaviour and residence time. CFD models often assume that when the inclusion reaches the slag layer it becomes entrapped without taking into account the possibility of it rebounding back into the steel. This assumption does not take into account the possibility of spontaneous emulsification as an inclusion undergoing these changes could take longer to float into the slag layer. When CFD models are being developed further, the possibility of spontaneous emulsification should be considered, especially for highly alloyed steels. A suggestion could be model the changing densities and viscosities as well as model a cloud of fine particles to see what can be done and what the model shows the outcome will be for these inclusions.

A mechanism that may be happening, such as inclusions bouncing back and oscillating for a period of time at the slag layer [82] cannot be measured due to the turbulent conditions in the continuous caster. Designing CFD models uses very complex fitting algorithms. The steelmaking process is extremely complicated, many different things (turbulence, fluid flow, and steel solidification to name a few) are occurring simultaneously especially in the continuous caster so some assumptions have to be made such as the behaviour when an inclusion reaches the slag layer. The findings from the literature review and the results shown, enables a building block to include these phenomena within a CFD model.

Understanding the complexities of inclusion behaviour, drives the need for developing CFD models further, both within current capabilities, but also the complexity and methodology of modelling itself. Tata Steel Europe have been installing a new direct strip mill within the IJmuiden plant, and with the reduced cross section, potential product portfolio, and up to date technology, the innovation, development and implementation of CFD models for this mill is the next step for producing quality products.

8.3.4 Innovative product design

New alloys are often designed to meet specific property requirements in a component. This requires knowledge of the composition, processing and microstructure. Traditional ways of developing new alloys were based on understanding of empirical relationships and modelling. The process of developing a new alloy is based on its potential physical properties. Many process issues could occur when moving from laboratory to an industrial scale. With the use of new software such as Thermo-Calc ® and MATLAB ® codes, there can be a more systematic approach for materials design to predict phase stability as a function of chemistry and temperature. The standard practice for alloy development is

shown in Figure 8.8 where compositions are calculated to meet specifications and this is carefully measured. The material is then cast in the desired mould, which is tailored to give suitable cooling rates. The material is then hot rolled to a thickness of around 3 mm (can depend on what product is being made). Any surface oxides are removed before cold rolling to a thickness of 1 mm. Further heat treatments are then completed such as annealing and ageing treatments before characterisation to give information on microstructures and chemical analysis. The final step is hardness and tensile testing.

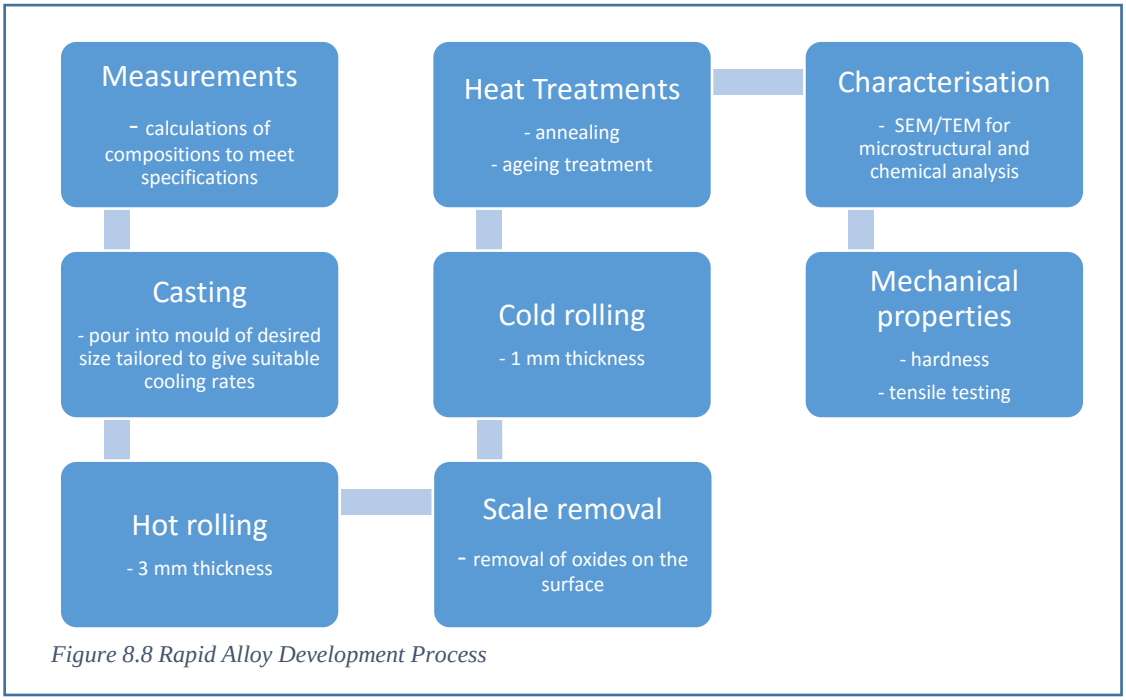

Figure 8.8 Rapid Alloy Development Process

The present findings show that for higher aluminium steels is would be advisable to understand the stability of the steel composition and what it will come into contact with in the steelmaking process such as the mould powder, refractory linings and the surrounding environment when the steel is transferred from the ladle to the mould. These dynamic calculations can be underpinned by the fundamental investigations studied in this project. Finding a matching mould flux and suitable refractory linings could be a part of early alloy development, potentially avoiding costly rabbit holes of investigation within an alloy development process. When suitable compositions are selected in the measurement phase, thermodynamic calculations could also be done simultaneously to check its compatibility with mould powders and the surrounding environment. This could save a lot of time and money in research and development, future developments for new alloys and product design. In this study, it has been shown that using a silica rich mould slag with a high aluminium steel causes spontaneous emulsification due to the reaction between the aluminium in the steel and the silica in the slag. However, a low aluminium steel of 0.04 wt. % does not cause spontaneous emulsification. The exact aluminium content in the steel to trigger and sustain an emulsion is currently unknown (between 0.04 wt. % and 1 wt. %) so before making a high aluminium steel, for example, this is something that would be useful to consider.

WMG, University of Warwick has a Rapid Allow Processing (RAP) facility where new alloys can be tested. Using these facilities could aid in designing a suitable mould powder by using the Vacuum Induction Melting furnace (VIM), and levitation drop furnace, to cast steel onto packed mould powder to study the reaction as the steel is solidifying. This could be repeated with different compositions of mould powder and steel.

9. Conclusions

The main objectives of this study were to determine the reaction kinetics between silica in the mould slag and aluminium in the steel through an innovative application of advanced laboratory techniques. The findings from this work have direct implication when considering the inclusion behaviour when casting steels.

The following conclusions have been drawn from the results presented:

1) The detection methods currently being employed to study inclusions is often 2D in nature, therefore the combination of techniques using HT-CLSM, XCT and SEM/EDS have allowed for the interactions between the inclusion and the steel to be examined in 3D with inclusions fully enclosed in molten steel.
2) Different test methods allowed for different aspects of the reaction and interaction to be investigated. The furnace tests allow for bulk equilibrium data and kinetic data to be found for the reaction between the mould powder and different grades of steel. The powder press samples showed the ability to embed an inclusion and the capabilities of using sintered steel to create a sample for this study. The pellet samples were useful when studying the reaction between the matrix and an entrained particle giving valuable information about the physical morphologies as well as chemical compositions. The dimple tests also gave kinetic data for potentially tracking inclusion compositions in the final slab against continuous casting processes and variable locations.
3) The kinetic study is useful for giving a time value for the equilibrium compositions of the steel and the inclusion to be reached assuming that the inclusion stays the same size (equilibrium is reached in 50 seconds). The mathematical model does give information into the rate limiting steps, mass transfer, and diffusion and reaction rates.
4) With the pellet samples, the inclusion reacted with aluminium in the 1 wt. % Al steel forming an emulsion after5 seconds and beginning to coalesce and reform into one particle by 20 seconds. This behaviour was not observed in the 0.04 Al wt. % steel. If an emulsion were to occur in the continuous caster, this would affect inclusion floatation times due to the compositional changes as well as morphology changes.

5) The dimple tests showed that a reaction does take place when the inclusion is liquid and the steel is semi-solid with the silica content decreasing to 35% of its starting composition after 20 seconds. The reaction was still ongoing but difficult to capture due to the steel becoming fully molten after 20 seconds. In the continuous caster, there are three possible reaction rates: when the steel is solid, mushy and liquid. If an inclusion is detected in the final product, based on the composition, the reaction time of the inclusion could be estimated.
6) The battery cans showed the defects were potentially caused by line defects or slag spots on the sheet steel before nickel coating and deep drawing. The direction of the parabolic lines is consistent with the direction of forming. It can be concluded that the inclusions found are not from the mould powder due to different compositions.
7) The above work provides a deeper understanding into the importance of mould flux design for high aluminium steels. Silica is an important component in mould fluxes due to its high viscosity and crystallisation properties and if silica were to be replaced for casting high aluminium steels, these properties still need to be maintained without a reaction taking place between the mould powder and the aluminium.

9.1. Summary of Innovation

The following aspects of innovation within the project have been defined as:

1) The combination of techniques (HT-CLSM, XCT, SEM/EDS) used to study the interactions and reactions between the inclusion and steel to find that spontaneous emulsification does occur due to the chemical potential between the silica in the inclusion and the aluminium in the steel.
2) Improved mould flux design for high-aluminium steels due to the reaction between silica in the slag and aluminium in the steel. There is an incentive to develop a less-reactive mould flux that still has the same properties of low viscosity and melting point, and crystallisation properties that will still continue to be appropriate for heat transfer and lubrication to produce a high quality slab with good surface quality,
3) Understanding the complexities of inclusion behaviour, drives the need for developing CFD models further, both within current capabilities, but also the complexity and methodology of modelling itself.
4) The results in this study can be used to analyse the defects in steel and inclusion compositions can be used to calculate how long the inclusion had reacted for and how long it had remained liquid. Inclusions on the surface or near the surface have a much lower reaction time in the liquid steel than an inclusion in the middle.

10. Future Work

The following points give suggestions for future work to build on the current findings within this project split into three categories:

10.1 Fundamental

1) At what Al content does emulsification actually occur? – The aluminium content of the steels that were tested were 0.04 wt. % and 1 wt. % and emulsification definitely occurs at 1 wt. %. Aluminium contents between these two compositions need to be tested to find out the concentration that triggers and sustains emulsification of an inclusion. This can be done with further HT-CLSM testing, XCT and SEM/EDS. To develop this further, the pellet samples could be made out of TWIP or TRIP steels to see what the inclusion reaction is like for a commercial material, as opposed to laboratory ideal cases
2) What happens if there are two inclusions? – The tests only examine one inclusion in bulk steel. If there were two inclusions, would emulsification happen to form one large inclusion or would these two inclusions go through the pathway for emulsification but stay separate? An example of how this could be carried out is through the use of an HDSv40 Gleeble sample. Figure 9.1 shows a potential sample design which has been modelled to provide a suitable hot zone within the centre section of the sample. This would allow the material to held, heated to the point of internal melting, and quenched for post mortem characterization.

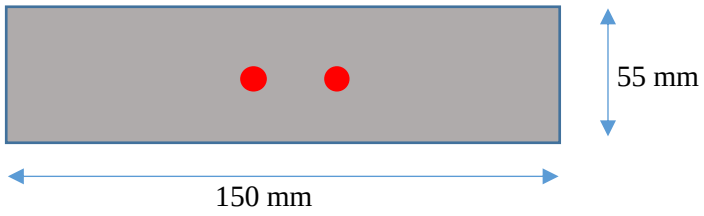

Figure 10.4 Potential sample design for the Gleeble tests where the red dots indicated the position of the inclusions that are 20 mm apart.

3) Further information for reaction kinetics for higher aluminium steels – at the moment, kinetic information on the slag-steel reaction is available for aluminium contents of up to 0.57 wt. %. The data can be extrapolated for higher aluminium concentrations in the steel but more accurate measurements will aid in calculating the residence time for inclusions and to study the exact material exchange. During this study, several attempts were made at attaining further information, however furnace, sample and experimental design has proved challenging. The learnings from this are included in Submission 3: *Artificial Inclusion Environments* –

Replicating Industry in the Laboratory. Building upon these initial findings to attain quality information would be invaluable to this field.

10.2 Scale-up

1) Mould flux design – finding a suitable composition of a mould flux that will be suitable for the production of high aluminium steels without compromising on viscosity and crystallisation, which are extremely important in continuous casting. Mould flux design is generally carried out by suppliers to steel companies. Development of fluxes suitable for highly alloyed steel would require an innovative approach to collaboration between the two stages of the supply chain in order to gain understanding of what is needed and the ability to produce the material in bulk and quality.

10.3 Plant

1) Access to TRIP and TWIP steels to study the inclusion patterns in the slab material and final product how they differ to the laboratory grade high aluminium steels. The compositions of the inclusions present could be compared to see if they align with the laboratory grades.
2) Battery cans – is there are a more automated way of checking defects in battery cans rather than manually checking for defects? Could these defects be prevented by making sure the surface is free from impurities that might be loosely attached to the surface before nickel plating it and deep drawing it?
3) The position of the inclusion in the slab can also give an indication to see if there is any difference in inclusion chemistry depending on the position through the thickness of the slab. This could indicate how long the inclusion has reacted with the steel.

References

1. Worldsteel. Sustainable Steel. At the core of a green economy. 40 (2012).
2. Steelmaking Process - an overview | ScienceDirect Topics. Available at: https://www.sciencedirect.com/topics/engineering/steelmaking-process. (Accessed: 25th February 2021)
3. Thomas, B. G., Yuan, Q., Mahmood, S., Liu, R. & Chaudhary, R. Transport and entrapment of particles in steel continuous casting. in *Metallurgical and Materials Transactions B: Process Metallurgy and Materials Processing Science* **45**, 22–35 (Springer, 2014).
4. Zhang, L. & Thomas, B. G. Inclusions in continuous casting of steel. *Proc. XXIV Natl. Steelmak. Symp.* 138–183 (2003).
5. Zhang, L. F. & Thomas, B. B. G. Inclusions in Continuous Casting of Steel. *XXIV Natl. Steelmak. Symp.* 138–183 (2003).
6. Liu, Z. & Li, B. Transient motion of inclusion cluster in vertical-bending continuous casting caster considering heat transfer and solidification. *Powder Technol.* **287**, 315–329 (2016).
7. Zhang, L. F. & Thomas, B. G. State of the Art in Evaluation and Control of Steel Cleanliness. *ISIJ Int.* **43**, 271–291 (2003).
8. ZHANG, L. feng. Indirect Methods of Detecting and Evaluating Inclusions in Steel-A Review. *J. Iron Steel Res. Int.* **13**, 1–8 (2006).
9. Zhang, X. *et al.* Characterization of the Three-Dimensional Morphology and Formation Mechanism of Inclusions in Linepipe Steels. *Metall. Mater. Trans. B Process Metall. Mater. Process. Sci.* (2017). doi:10.1007/s11663-016-0833-4
10. Ren, Y. *et al.* Detection of non-metallic inclusions in steel continuous casting billets. *Metall. Mater. Trans. B Process Metall. Mater. Process. Sci.* **45**, 1291–1303 (2014).
11. Pretorius, E. B., Oltmann, H. G. & Schart, B. T. An overview of steel cleanliness from an industry perspective. in *Iron and Steel Technology* (2015).
12. Sutcliffe, N. Slag / refractory and metal / refractory interactions during the production of stainless steels. *VII Int. Conf. Molten Slags Fluxes Salts* **5**, 423–436 (2004).
13. Efendy, H., Safarudin, M. & Sihombing, H. Molten Metal-Slag-Refractory Reactions During Converting Process. *Int. J. Eng. Technol. IJET-IJENS* **10**, 40–43 (2010).
14. HAN, Z. *Mechanism and Kinetics of Transformation of Alumina Inclusions By Calcium Treatment*. *Acta Metallurgica Sinica (English Letters)* **19**, (2006).
15. Zhang, L. & Thomas, B. G. Inclusion investigation during clean steel production at Baosteel. *ISS Tech 2003* **2003**, 141–156 (2003).
16. ABOUT STEEL | worldsteel. Available at: https://www.worldsteel.org/about-steel.html. (Accessed: 25th February 2021)
17. World Steel Association. Wolrd Steel in Figures 2015 - Abreviated. *World steel Assoc.* 3–30 (2015). doi:https://www.worldsteel.org/dms/internetDocumentList/bookshop/2015/World-Steel-in-Figures-2015/document/World%20Steel%20in%20Figures%202015.pdf
18. World Steel Association. Steel Statistical Yearbook 2019 Concise version. *World Steel Assoc.* 1–6 (2019).

19. Fruehan, R. J. Overview of Steelmaking Processes and Their Development. *Making, Shap. Treat. steel - Steelmak. Refin. Vol.* 1–12 (1998).

20. Cho, J.-W. *et al.* Assessment of CaO-Al2O3 Based Mold Flux System for High Aluminum TRIP Casting. *Isij Int.* **53**, 62–70 (2013).

21. Matsumiya, T. Steelmaking technology for a sustainable society. *Calphad* **35**, 627–635 (2011).

22. Park, J. H. & Kang, Y. Inclusions in Stainless Steels − A Review. *Steel Res. Int.* **88**, 1–26 (2017).

23. Fekete, J. R. & Hall, J. N. *Design of auto body: Materials perspective*. *Automotive Steels: Design, Metallurgy, Processing and Applications* (Elsevier Ltd, 2016). doi:10.1016/B978-0-08-100638-2.00001-8

24. Mohanty, O. N. 13 – Forging Grade Steels for Automotives. in *Automotive Steels* 413–453 (2017). doi:10.1016/B978-0-08-100638-2.00013-4

25. 5 Reasons Why It's Important To Recycle Metals | Axil Integrated Services. Available at: https://axil-is.com/five-reasons-why-its-important-to-recycle-metals/. (Accessed: 28th February 2021)

26. Poirier, J. A review: influence of refractories on steel quality. *Metall. Res. Technol.* **112**, 410 (2015).

27. Wang, W., Lu, B. & Xiao, D. A Review of Mold Flux Development for the Casting of High-Al Steels. *Metall. Mater. Trans. B Process Metall. Mater. Process. Sci.* **47**, 384–389 (2016).

28. Holappa, L. E. K. & Helle, A. S. Inclusion Control in High-Performance Steels. *J. Mater. Process. Tech.* **53**, 177–186 (1995).

29. Smil, V. Modern Ironmaking and Steelmaking. *Still Iron Age* 87–114 (2016). doi:10.1016/B978-0-12-804233-5.00005-1

30. WorldSteel. Steel Statistical Yearbook 2010. (2010).

31. Holappa, L. *Secondary Steelmaking*. *Treatise on Process Metallurgy* **3**, (2014).

32. Louhenkilpi, S. Chapter 1.8 – Continuous Casting of Steel. in *Treatise on Process Metallurgy* 373–434 (2014). doi:10.1016/B978-0-08-096988-6.00007-9

33. Väinölä, R. V., Holappa, L. E. K. & Karvonen, P. H. J. Modern steelmaking technology for special steels. *J. Mater. Process. Tech.* **53**, 453–465 (1995).

34. ZHANG, L. feng. Inclusion and Bubble in Steel-A Review. *J. Iron Steel Res. Int.* **13**, 1–8 (2006).

35. Zhang, L. *et al.* Investigation of fluid flow and steel cleanliness in the continuous casting strand. *Metall. Mater. Trans. B Process Metall. Mater. Process. Sci.* **38**, 63–83 (2007).

36. Tervo, H., Kaijalainen, A., Pikkarainen, T., Mehtonen, S. & Porter, D. Effect of impurity level and inclusions on the ductility and toughness of an ultra-high-strength steel. *Mater. Sci. Eng. A* **697**, 184–193 (2017).

37. Dekkers, R. *et al.* Non-metallic inclusions in aluminium killed steels. *Ironmak. Steelmak.* **29**, 437–444 (2002).

38. Ernesto RAMIREZ LOPEZ, P., Nazem JALALI, P., Björkvall, J., Sjöström, U. & Nilsson, C. Recent Developments of a Numerical Model for Continuous Casting of Steel: Model Theory, Setup and Comparison to Physical Modelling with Liquid Metal. *ISIJ Int.* **54**, 342–350 (2014).

39. Monaghan, B. J. *et al.* Effect of Slag Composition on Wettability of Oxide Inclusions. *ISIJ Int.* **55**, 1834–1840 (2015).

40. Emi, T. Improving steelmaking and steel properties. in *Fundamentals of Metallurgy* 503–554 (Elsevier Inc., 2005). doi:10.1533/9781845690946.2.503

41. Riyahimalayeri, K. *Slag , Steel , Ladle and Non-metallic Inclusions Equilibria in an ASEA-SKF Ladle Furnace*. (2012).

42. Park, J., Sridhar, S. & Fruehan, R. J. Ladle and Continuous Casting Process Models for Reduction of SiO2 in SiO2-Al2O3-CaO Slags by Al in Fe-Al(-Si) Melts. *Metall. Mater. Trans. B Process Metall. Mater. Process. Sci.* **46**, 109–118 (2014).

43. Fernandes, M., Cheung, N. & Garcia, A. Investigation of nonmetallic inclusions in continuously cast carbon steel by dissolution of the ferritic matrix. *Mater. Charact.* **48**, 255–261 (2002).

44. Pires, J. C. S. & Garcia, A. Study of the nature of non-metallic inclusions in samples of aluminum and silicon killed low carbon steels, collected in the refining treatment and continuous casting stages. *Mater. Res.* **7**, 517–521 (2004).

45. Bannenberg, N. Demands on refractory material for clean steel production. *Glob. Dev. Refactories* 36–59 (1995).

46. Turkdogan, E. T. & Fruehan, R. J. Fundamentals of Iron and Steelmaking. *Steelmak. Refin. Vol.* **i**, 13–157 (1998).

47. Yin, H. H. B., Shibata, H., Emi, T. & Suzuki, M. 'In-situ' Observation of Collision, Agglomeration and Cluster Formation of Alumina Inclusion Particles on Steel Melts. *ISIJ Int.* **37**, 936–945 (1997).

48. Tervo, H., Kaijalainen, A., Pikkarainen, T., Mehtonen, S. & Porter, D. EFFECT OF IMPURITY LEVEL AND INCLUSIONS ON THE DUCTILITY AND TOUGHNESS OF AN ULTRA-HIGH-STRENGTH STEEL. *Mater. Sci. Eng. A* (2017). doi:10.1016/j.msea.2017.05.013

49. Imagumbai, M. & Takeda, T. Influence of Calcium-treatment on Sulfide- and Oxide-inclusions in Continuous-cast Slab of Clean Steel - Dendrite Structure and Inclusions. *ISIJ Int.* **34**, 574–583 (1994).

50. Lino, R. E. *et al.* Influence of the chemical composition on steel casting performance. *J. Mater. Res. Technol.* **6**, 1–7 (2016).

51. Yang, J., Wang, X. H., Jiang, M. & Wang, W. J. Effect of calcium treatment on non-metallic inclusions in ultra-low oxygen steel refined by high basicity high Al2O3slag. *J. Iron Steel Res. Int.* **18**, 8–14 (2011).

52. Lino, R. E. *et al.* Influence of the chemical composition on steel casting performance. *J. Mater. Res. Technol.* **6**, 50–56 (2017).

53. Park, J., Sridhar, P. S. & Fruehan, P. R. J. Activity of SiO 2 in SiO 2 -Al 2 O 3 -CaO Slags in Equilibrium With Fe-Al Melts. *AISTech - Iron Steel Technol. Conf. Proc.* 2177–2184 (2012). doi:10.1007/s11663-014-0076-1

54. Park, J., Sridhar, S. & Fruehan, R. J. Activity coefficient of SiO2in SiO2-Al2O3-CaO Slags with Low SiO2-content at 1873 K (1600 C). *Metall. Mater. Trans. B Process Metall. Mater. Process. Sci.* **44**, 13–15 (2013).

55. Hibbeler, L. C. & Thomas, B. G. Mold slag entrainment mechanisms in continuous casting molds. *Iron Steel Technol.* **10**, 121–136 (2013).

56. Rackers, K. & Thomas, B. 78th Steelmaking Conf. *Proc., ISS, Warrendale, PA* (1995).

57. Rackers, K. G. & Thomas, B. G. Clogging in Continuous Casting Nozzles. *78th Steelmak. Conf. Proc.* **78**, 723–734 (1995).

58. Hamilton, L. T. Technical Note - The Introduction of “Slit” Submerged Entry Nozzles to No. 1 Slab Caster, BHP International Group Pt. Kembla, NSW. *Bull. Proc. Austras. Inst. Min. Met.* **290**, 75–78 (1985).

59. Haers, F. First Experience in Using the Caster Tube Change Device (TCD90). in *Fourth International Conference on Continuous Casting* 1988 (1988).

60. Schmidt, M., Russo, T. J. & Bederka, D. J. Steel Shrouding and Tundish Flo w Control to Improve Cleanliness and Reduce Plugging. in *73rd ISS Steelmaking Conference, Detroit, MI* (1990).

61. Mizoguchi, T., Ueshima, Y., Sugiyama, M. & Mizukami, K. Influence of Unstable Non-equilibrium Liquid Iron Oxide on Clustering of Alumina Particles in Steel. *Tetsu-to-Hagane* **99**, 601–609 (2013).

62. Monroe, R. Porosity in castings. *AFS Trans* **5**, 10 (2005).

63. Atzema, E. H. *Formability of auto components*. *Automotive Steels: Design, Metallurgy, Processing and Applications* (Elsevier Ltd, 2016). doi:10.1016/B978-0-08-100638-2.00003-1

64. Ghosh, P. & Ray, R. K. *Deep drawable steels*. *Automotive Steels: Design, Metallurgy, Processing and Applications* (Elsevier Ltd, 2016). doi:10.1016/B978-0-08-100638-2.00005-5

65. Chen, L., Malfliet, A., Jones, P. T., Blanpain, B. & Guo, M. Degradation mechanisms of alumina–silica runner refractories by carbon steel during ingot casting process. *Ceram. Int.* **42**, 10209–10214 (2016).

66. Duderstadt, G. C., Iyengar, R. K. & Matesa, J. . Tundish Nozzle Blockage in Continuous Casting. *J. Met.* 89–94 (1968).

67. Hoh, B. Improvement of Cleanliness in Continuous Casting. in *Fourth International Conference on Continuous Casting, 1988.* 1988 (1988).

68. Choudhary, S. K. Influence of Modified Casting Practice on Steel Cleanliness. *ISIJ Int.* **51**, 557–565 (2011).

69. Hansen, T. & Jonsson, P. Electric Furnace. in *Electric Furnace Conference Proceedings, ISS, Warrendale, PA* 59, 71–81 (2001).

70. Baker, T. J. & Charles, J. A. Effect of Second-Phase Particles on the Mechanical Properties of Steel. in *Effect of Second-Phase Particles on the Mechanical Properties of Steel* 8–94 (1971).

71. Grethen, E. & Philipe, L. The Iron and Steel Institute, London, Balatonfured, Hungary, (1970), 29-34. in *Production and Application of Clean Steels* 29–34 (1970).

72. Sulasalmi, P., Visuri, V. V., Kärnä, A. & Fabritius, T. Simulation of the effect of steel flow velocity on slag droplet distribution and interfacial area between steel and slag. *Steel Res. Int.* **86**, 212–222 (2015).

73. Olette, M. & Gatellier, C. Information Symposium of Casting and Solidification of Steel. in *Information Symposium of Casting and Solidification of Steel* 1977 (1977).

74. Zhang, L., Thomas, B. G., Wang, X. & Cai, K. Evaluation and Control of Steel Cleanliness: Review. *85th Steelmak. Conf. ISS-AIME, Warrendale,PA* 431–452 (2002).

75. Bartosiaki, B. G., Pereira, J. A. M., Bielefeldt, W. V. & Vilela, A. C. F. Assessment of inclusion analysis via manual and automated SEM and total oxygen content of steel. *J. Mater. Res. Technol.* **4**, 235–240 (2015).

76. Harris, M. L. A study on non-metallic inclusions in foundry steel process. *ProQuest Diss. Theses* 94 (2016).

77. Eckel, J. A., Glaws, P. C., Wolfe, J. O. & Zorc, B. J. Clean engineered steels - progress at the end of the twentieth century. in *1998 Symposium on Advances in the Production and Use Steel with Improved Internal Cleanliness* 1–11 (ASTM Special Technical Publication, 1998).

78. Bastien, P. The possibilities and limitations of ultrasonics in the non-destructive testing of steel. *NDT Int.* **10**, 297–305 (1977).

79. Wells, J. M. Quantitative XCT evaluation of porosity in an aluminum alloy casting. *TMS Annu. Meet.* 77–84 (2007).

80. Atkinson, H. V. & Shi, G. Characterization of inclusions in clean steels: A review including the statistics of extremes methods. *Prog. Mater. Sci.* **48**, 457–520 (2003).

81. Kountouriotis, Z. Modelling of the liquid slag behaviour in the continuous casting mould. *PQDT - UK Irel.* (2011).

82. Shannon, G., White, L. & Sridhar, S. Modeling inclusion approach to the steel/slag interface. *Mater. Sci. Eng. A* **495**, 310–315 (2008).

83. Chung, Y. & Cramb, A. W. Direct observation of spontaneous emulsification and associated interfacial phenomena at the slag–steel interface. *Philos. Trans. R. Soc. London. Ser. A Math. Phys. Eng. Sci.* **356**, 981–993 (1998).

84. Assis, A. N. *et al.* Spontaneous Emulsification of a Metal Drop Immersed in Slag Due to Dephosphorization: Surface Area Quantification. *Metall. Mater. Trans. B Process Metall. Mater. Process. Sci.* **46**, 568–576 (2015).

85. Spooner, S. *et al.* Investigation into the Cause of Spontaneous Emulsification of a Free Steel Droplet; Validation of the Chemical Exchange Pathway. *Metall. Mater. Trans. B Process Metall. Mater. Process. Sci.* **47**, 2123–2132 (2016).

86. Tacke, K. H. Overview of Particles and bubbles in continuously cast steel. *J. Iron Steel Res. Int.* **18suppleme**, 211–219 (2011).

87. Woodruff, D. P. How does your crystal grow? A commentary on Burton, Cabrera and Frank (1951) 'The growth of crystals and the equilibrium structure of their surfaces'. *Philosophical Transactions of the Royal Society A: Mathematical, Physical and Engineering Sciences* **373**, (2015).

88. Mu, W., Dogan, N. & Coley, K. S. In Situ Observations of Agglomeration of Non-metallic Inclusions at Steel/Ar and Steel/Slag Interfaces by High-Temperature Confocal Laser Scanning Microscope: A Review. *JOM* **70**, 1199–1209 (2018).

89. Yin, H., Shibata, H., Emi, T. & Suzuki, M. Characteristics of Agglomeration of Various Inclusion Particles on Molten Steel Surface. *ISIJ Int.* **37**, 946–955 (1997).

90. Sharan, A. & Cramb, A. W. Interfacial Tensions of Liquid Fe-Ni Alloys and Stainless Steels in Contact with CaO-SiO2-AI203-Based Slags at 1550 ~. **26**, 87–94 (1995).

91. Rhamdhani, M. A., Brooks, G. A. & Coley, K. S. Kinetics of metal/slag reactions during spontaneous emulsification. *Metall. Mater. Trans. B Process Metall. Mater. Process. Sci.* **36**, 219–227 (2005).

92. Brooks, G. A., Rhamdhani, M. A., Coley, K. S. & Pan, Y. Transient Kinetics of Slag Metal Reactions. **40**, 353–362 (2009).

93. Rhamdhani, M. A., Brooks, G. A. & Coley, K. S. Kinetics of Metal / Slag Reactions during Spontaneous Emulsification. **36**, (2005).

94. Shefer, E. *et al.* State of the Art of CT Detectors and Sources: A Literature Review. *Curr. Radiol. Rep.* **1**, 76–91 (2013).

95. Scanning Electron Microscopy (SEM). Available at: https://serc.carleton.edu/research_education/geochemsheets/techniques/SEM.html. (Accessed: 6th March 2019)

96. Zhang, L., Aoki, J. & Thomas, B. G. Inclusion removal by bubble flotation in a continuous casting mold. *Metall. Mater. Trans. B* **37**, 361–379 (2006).

97. Raviraj, A. *et al.* The Spontaneous Emulsification of Entrained Inclusions During Casting of High Aluminum Steels. *Metall. Mater. Trans. B* doi:10.1007/s11663-021-02091-z

98. Gaye, H., Lucas, L. D., Olette, M. & Riboud, P. V. Metal-slag interfacial properties: Equilibrium values and 'dynamic' phenomena. *Can. Metall. Q.* **23**, 179–191 (1984).

99. Cowles, J. H. Kinetics and Thermodynamics of Chemical reactions in Aqueous Solutions. (1990).

100. Hino, Mitsutaka; Ito, K. *Thermodynamic data for steelmaking*. (Tohoku University Press, 2010).

101. Spooner, S., Warnett, J. M., Bhagat, R., Williams, M. A. & Sridhar, S. Calculating the macroscopic dynamics of gas/metal/slag emulsion during steelmaking. *ISIJ Int.* **56**, 2171–2180 (2016).

102. Khurana, B., Spooner, S., Rao, M. B. V., Roy, G. G. & Srirangam, P. In situ Observation of Calcium Oxide Treatment of Inclusions in Molten Steel by Confocal Microscopy. *Metall. Mater. Trans. B Process Metall. Mater. Process. Sci.* **48**, 1409–1415 (2017).

103. Zhang, L., Thomas, B. G., Wang, X. & Cai, K. Evaluation and Control of Steel Cleanliness: Review. *85th Steelmak. Conf. ISS-AIME*, 431–452 (2002). doi:10.1074/jbc.M804001200

104. Spooner, S., Assis, A. N., Warnett, J., Fruehan, R. & Williams, M. A. CTSSC-EMI Symposium CSLM , XCT Couple Interrogation of the Emulsification Interaction between Free Steel Droplets Suspended in Steel Making Slags . 3–4 (2015).

105. Silva, A. C. Interaction parameters of oxygen and deoxidants in liquid iron. *J. Min. Metall. Sect. B Metall.* **52**, 41–46 (2016).

106. Ghosh, A. *Secondary Steelmaking Principles and Applications*. *CRC Press* (2001).

107. Thornton, P. A. The influence of nonmetallic inclusions on the mechanical properties of steel: A review. *J. Mater. Sci.* **6**, 347–356 (1971).

108. You, D., Michelic, S. K., Presoly, P., Liu, J. & Bernhard, C. Modeling Inclusion Formation during Solidification of Steel: A Review. *Metals (Basel).* **7**, 460 (2017).

109. Maciejewski, J. The Effects of Sulfide Inclusions on Mechanical Properties and Failures of Steel Components. *J. Fail. Anal. Prev.* **15**, 169–178 (2015).

110. Yan, Wei; McLean, Alexander; Yang, Yindong; Chen, Weiqing; Barati, M. Evaluation of mold flux for continuous casting of high-aluminium steel. in *Advances in Molten Slags, Fluxes, and Salts: Proceedings of The 10th International Conference on Molten Slags, Fluxes and Salts (MOLTEN16)* (ed. Reddy, Ramana G.; Chaubal, Pinakin; Pistorius, P. Chris; Pal, U.) 279–290 (2016).

111. Shi, Chengbin; Seo, Myung-Duk; Cho, Jungwook; Kim, S.-H. Crystallization characteristics of CaO-Al2O3-based mold flux and their effects on in-mold performance during high-aluminum TRIP steels continuous casting. *Metall. Mater. Trans. B Process Metall. Mater. Process. Sci.* **45**, 1081–1097 (2016).

112. Lu, B.X.; Wang, W. . Effects of fluorine and BaO on the crystallization behavior of lime-alumina-based mold flux for casting high-Al steels. *Metall. Mater. Trans. B* **46**, 852–862 (2016).

113. Effect Ironed of Non-metallic Can from Inclusion of Flange Cracking of Drawn and Tinplate * By Hideo KOBAYASHI ,** Teruo KUROKAWA ,** Takayoshi SHIMOMURA ,** Kazuo MATSUDO ** and Shinobu MIYAHARA **. 410–416 (1983).